

Applications of Variable Speed Control for Contending with Recurrent Highway Congestion



**Morgan State University
The Pennsylvania State University
University of Maryland
University of Virginia
Virginia Polytechnic Institute & State University
West Virginia University**

**The Pennsylvania State University
The Thomas D. Larson Pennsylvania Transportation Institute
Transportation Research Building ❖ University Park, PA 16802-4710
Phone: 814-865-1891 ❖ Fax: 814-863-3707
www.mautc.psu.edu**

1. Report No. UMD-2012-03	2. Government Accession No.	3. Recipient's Catalog No.	
4. Title and Subtitle Applications of Variable Speed Control for Contending with Recurrent Highway Congestion		5. Report Date July 21, 2014	
		6. Performing Organization Code	
7. Author(s) Mark L. Franz and Gang-Len Chang		8. Performing Organization Report No.	
9. Performing Organization Name and Address University of Maryland College, Park, Maryland		10. Work Unit No. (TRAIS)	
		11. Contract or Grant No. DTRT12-G-UTC03	
12. Sponsoring Agency Name and Address US Department of Transportation Research & Innovative Technology Admin UTC Program, RDT-30 1200 New Jersey Ave., SE Washington, DC 20590		13. Type of Report and Period Covered Final	
		14. Sponsoring Agency Code	
15. Supplementary Notes			
16. Abstract <p>This research project developed vital operational guidelines for design of a variable speed limit (VSL) system and its integrated operations with ramp metering control in contending with recurrent highway congestion. The developed guidelines can serve as an effective tool for traffic engineers to determine when to activate a VSL control and under what traffic conditions it needs to be supplemented by ramp metering operations to ensure the stability of traffic evolution over the congested highway segment. This report also presents various measures of effectiveness for evaluating the benefits of VSL and its integration with ramp metering control. A VSL control algorithm to compute the time-varying speeds in real time, based on detected traffic conditions, was developed in this study. Extensive simulation experiments, calibrated with the field data from US100 in Maryland, were conducted to evaluate the effectiveness of the developed VSL algorithm. Both the experimental results and sensitivity analyses with respect to key model parameters confirmed that proper implementation of VSL can indeed mitigate the congestion caused by the high-speed variance among vehicles and allow traffic flows to better utilize the available roadway capacity.</p>			
17. Key Words VSL, ramp metering, integration, recurrent congestion.		18. Distribution Statement No restrictions. This document is available from the National Technical Information Service, Springfield, VA 22161	
19. Security Classif. (of this report) Unclassified	20. Security Classif. (of this page) Unclassified	21. No. of Pages 93	22. Price

Acknowledgements

The authors of this manuscript would like to thank the MAUTC for the funding of this research. In addition, we would also like to thank the Maryland State Highway Administration for their invaluable feedback throughout the course of this research.

Disclaimer

The contents of this report reflect the views of the authors, who are responsible for the facts and the accuracy of the information presented herein. This document is disseminated under the sponsorship of the U.S. Department of Transportation's University Transportation Centers Program, in the interest of information exchange. The U.S. Government assumes no liability for the contents or use thereof.

Table of Contents

1. Problem Statement	1
1.1. Introduction.....	1
1.2. Literature Review.....	4
1.2.1. Bottlenecks and the Effect of VSL on Traffic Flow.....	4
1.2.2. VSL in Recurrent Congestion.....	9
2. Research Objectives.....	17
2.1. Research Motivation	17
2.2. Scope and Objectives.....	19
2.3. Organization.....	22
3. Methodology	22
3.1. Optimal VSL Control.....	22
3.2. VSL Control with Ramp Metering	34
3.2.1. General VSL Control Logic	34
3.2.2. VSL System Activation	36
3.2.3. VSL System Activation	37
3.2.4. Supplemental Ramp Metering Control Algorithm	42
3.2.5. Ramp Metering Activation	47
3.2.6. Ramp Queue Override and Ramp Metering Rate.....	50
3.2.7. Upstream Ramp Metering Supplementation	52
3.2.8. Ramp Metering De-Activation	55
3.3. Statistical Models for VSL and VSL with Ramp Metering Benefits.....	56
3.3.1. Measures of Effectiveness for VSL Control.....	56
3.3.2. Simulation Calibration.....	59
3.3.3. Data Set Development	60
3.3.4. Simulation Calibration.....	62
3.3.5. VSL Benefits Models	64

4. Findings.....	67
4.1. Optimal VSL Control Results.....	67
4.2. VSL and VSL with Ramp Metering Benefits Models Results.....	71
4.2.1. Hierarchical Model Results and Analysis.....	71
4.2.2. DC Model Results and Analysis.....	75
5. Conclusions.....	78
5.1. Optimal VSL Control Algorithms.....	78
5.2. VSL Model Comparison.....	78
5. Recommendations.....	79

List of Figures

Figure 1-1: VSL Gantry Display	2
Figure 1-2: VSL Displayed on a VMS.....	2
Figure 1-3: Roadside Electronic Speed Limit Signs (Mandatory and Advisory)	3
Figure 2-1: Effect of VSL on the Flow-Density Diagram (Carlson et al. 2011)	7
Figure 3-1. Typical Freeway Segments	23
Figure 3-2: An Illustration of Kalman Filter Correction and Update Process.....	29
Figure 3-3: Example of the VSL Control Strategy	31
Figure 3-4. Flow Chart of the Enhanced Proactive Model VSL Control System.....	33
Figure 3-5: VSL Control Operational Flow Chart	36
Figure 3-7: Ramp Metering Activation.....	49
Figure 3-8: Map of Base Scenario, MD100 (Google Maps, 2013)	60
Figure 3-9: Hierarchical Structure of Planning Model.....	65
Figure 4-1(A). Time-dependent Travel Time: BASIC-TTT, KF-TTT vs. No-VSL Scenario.....	69
Figure 4-1(B). Time-dependent Travel Time: BASIC-SV, KF-SV vs. No-VSL Scenario....	69
Figure 4-1(C). Time-dependent Travel Time: KF-TTT, KF-SV vs. No-VSL Scenario	69
Figure 4-2(A). Time-dependent Number of Stops: BASIC-TTT, KF-TTT vs. No-VSL Scenario.....	70
Figure 4-2(B). Time-dependent Number of Stops: BASIC-SV, KF-SV vs. No-VSL Scenario.....	70
Figure 4-2(C). Time-dependent Number of Stops: KF-TTT, KF-SV vs. No-VSL Scenario.....	70

List of Tables

Table 3-1: Final List of Control Variables for Model Development	61
Table 3-2. The Calibration Results of Parameters	63
Table 4-1. Performance Comparison between Different Scenarios	72
Table 4-2: Change in Speed Variance Modeling Results in the Hierarchical Structure	72
Table 4-3: Change in Speed Variance Modeling Accuracy in the Hierarchical Structure..	73
Table 4-4: Change in Total Time Spent Modeling Results in the Hierarchical Structure ..	74
Table 4-5: DC Modeling Results.....	76
Table 4-6: DC Modeling Results.....	77

1. Problem Statement

1.1. Introduction

Traffic demand increases are pushing aging ground transportation infrastructures to their theoretical capacity. The result of this demand is traffic bottlenecks that are a major cause of delay on urban freeways. In addition, the queues associated with those bottlenecks increase the probability of a crash while adversely affecting environmental measures such as emissions and fuel consumption. With limited resources available for network expansion, traffic professionals have developed active traffic management system (ATMS) in an attempt to mitigate the negative consequences of traffic bottlenecks. Among these ATMS strategies, variable speed limits (VSL) have been gaining international interest for their potential to improve safety, mobility, and environmental measures at freeway bottlenecks.

VSLs are speed limits that can change based on real-time traffic and/or weather conditions (Fuhs, 2012). The changed speed limits are communicated to road users in a number of ways, including overhead gantries (Figure 1-1), variable message signs (Figure 1-2), and electronic roadside speed limit signs (Figure 1-3). The activation of the VSL system and the control logic for setting the VSL may be controlled manually by a traffic management center (TMC) or by using real-time traffic data as part of an intelligent transportation system (ITS). As evident from Figure 3, the VSL may be mandatory or advisory. In any case, the primary objective of VSL is to harmonize the traffic flow near a bottleneck. This harmonization is most commonly accomplished by gradually reducing the speed limit on the segment upstream of the bottleneck. In doing so, the shockwaves associated with vehicle deceleration are suppressed, resulting in improved traffic flow and safety. Other potential benefits of VSL

include delayed onset of the bottleneck formation, shorter duration of a congestion period, and better utilized capacity of the controlled corridor.



Figure 1-1: VSL Gantry Display



Figure 1-2: VSL Displayed on a VMS

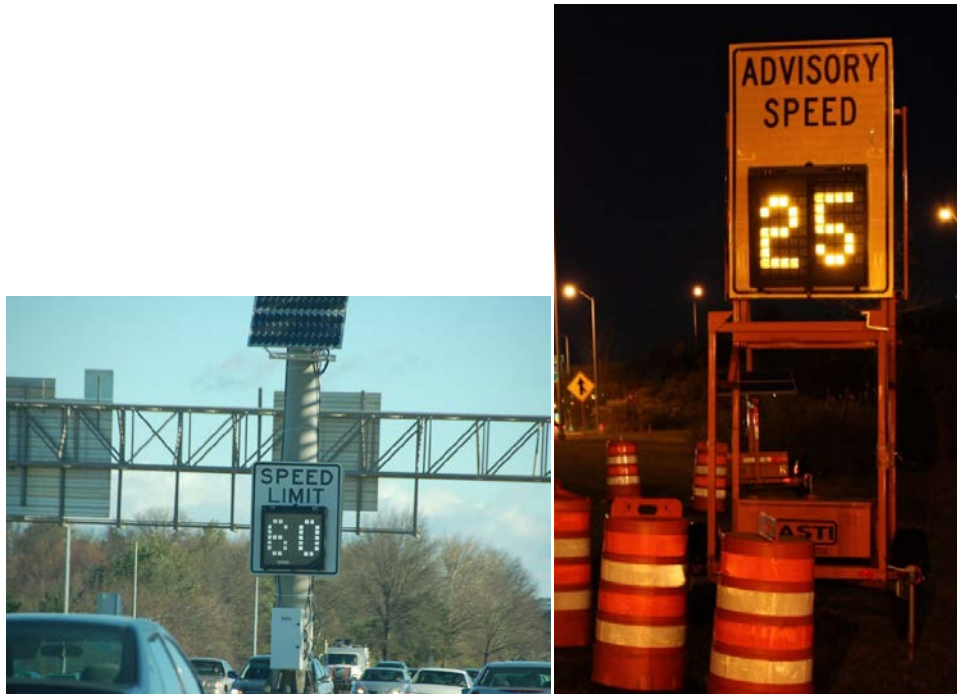


Figure 1-3: Roadside Electronic Speed Limit Signs (Mandatory and Advisory)

Interestingly, VSL has been used to improve traffic flow for several decades. In fact, the first VSL system in the United States was installed near Detroit, Michigan in 1962 (Robinson, 2000), with the goal of alerting motorists to decelerate when approaching a bottleneck and accelerating after passing the bottleneck. Since then, several other states and countries have experimented with the use of VSL on freeways. These field studies offer valuable insight on the potential of VSL to remedy the adverse effects of traffic bottlenecks. However, advancements in traffic simulation software are allowing practitioners and researchers alike to evaluate traffic management strategies, such as VSL, in the planning phase. This methodology serves as an alternative to time-consuming and often expensive field

observations. Using simulation, several VSL deployment strategies have been developed for specific applications such as inclement weather conditions, work zones, and recurrent congestion. Additionally, some recurrent congestion studies have investigated the pairing of VSL with ramp metering. Nevertheless, the objectives, implementation scheme, and evaluation methods vary from study to study.

1.2. Literature Review

1.2.1. Bottlenecks and the Effect of VSL on Traffic Flow

Traffic bottlenecks are segments with a reduced traffic flow rate that may be caused by changes in road geometry (i.e., lane drop), adverse driving conditions (i.e., snow/ice), or an area of intense weaving (i.e., freeway on/off ramps). Regardless of the cause, the formation of a bottleneck can reduce the mobility and safety of the local network. To better understand how bottlenecks are formed, Kerner and Reborn (1997 and 2002) and Kerner (2002) investigated traffic characteristics near a bottleneck created near an on-ramp. The work produced a three-phase traffic flow model to describe observed phenomena at bottlenecks. The researchers argued that moving jams emerge from a synchronized flow state and cannot occur in free-flow conditions. At on-ramps with high flow rates, a synchronized flow pattern is created upstream of the ramp, allowing for jams to occur if the density continues to increase. The recognition of synchronized flow rates has become an important part of many advanced VSL control algorithms that use predictive modeling to intervene before jam conditions are created. Additional work on the effect of speed limits on bottleneck formation

was done by Sailer et al. (1997). This research generated a mathematical formula of the speed-density relationship as a function of speed limits near bottlenecks. This relationship proved that speed limits can affect the formation of bottlenecks and the propagation of traffic jams. The research of Bellmans et al. (2003) and Ghods et al. (2010) recommended that a merging term is needed to estimate the speeds near an on-ramp because the observed behavior could be explained by increased density alone. The requirement for this term arises from lane-changing and weaving behavior in the proximity of an on-ramp. Lastly, Barlovic et al. (1998) proposed the slow-to-start rule that describes the phenomenon that vehicles tend to accelerate at a slow rate when exiting a high-density segment.

With a reasonable understanding of the formation of bottlenecks, several researchers have moved to investigate the impact of VSL on the fundamental diagrams. Papageorgiou et al. (2008) explored the effects of VSL on traffic flow by comparing the flow-occupancy curves for different speed limits. The authors found that at under critical densities VSL flattens the slope of the flow-occupancy diagram and shifts the critical occupancy to a higher value. In relation, the research by Nissan and Koutsopoulos (2011) evaluated the effectiveness of VSL using level of service under several control scenarios. Interestingly, the researchers found that the definition of level of service was dependent on the implemented traffic controls. A similar finding was discovered by Wang and Ioannou (2011), reporting that the change of speed limit for a long period, as would be the case in inclement weather or long-term work zones, can change the shape of the fundamental diagram. Kononov et al. (2012) investigated the relationship between flow/density, speed, and crash rate using neural

networks. This relationship was used to calculate a Flow Crash Potential Indicator under various conditions. The study found that the crash rates remain constant until a critical threshold of speed and density was achieved. Using this observed threshold, a VSL control algorithm was proposed with the objective of improving traffic safety. However, the effects of the algorithm were not tested in this study. Further research on the effect of VSL on traffic flow was conducted by Kianfar et al. (2013), who investigated the operational impacts of a field-deployed VSL system on I-270 in the State of Missouri. Statistical tests showed that the flow-occupancy diagram changed significantly under VSL control in seven of eight congested locations. The slopes of the flow-occupancy function at over-critical occupancies were steeper under VSL control. However, the study found some inconsistencies in the effect of VSL on some traffic flow parameters such as the direction of critical occupancy shift and the duration of the congested period.

Lastly, the work of Carlson et al. (2011) showed the impact of VSL on fundamental traffic flow relationships, as illustrated in Figure 2-1. As shown in Figure 2-1(a), at under-critical densities VSL will reduce flow. However, Figure 2-1(b) shows that at over-critical densities, VSL can improve traffic flow. In Figure 2-1(b), each curve represents the fraction of the original speed limit (e.g., $b = 0.8$ represents 80% of the original speed limit). Thus, for a given over-critical density there exists a speed limit that maximizes flow.

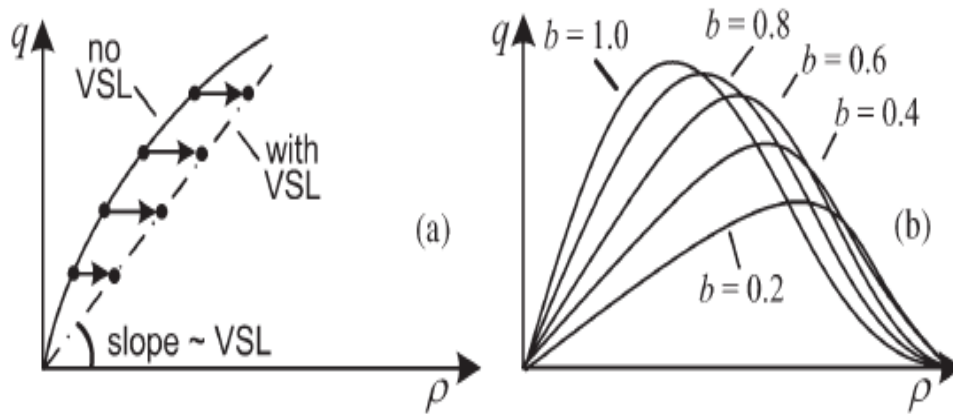


Figure 2-1: Effect of VSL on the Flow-Density Diagram (Carlson et al. 2011)

In addition to the effect of VSL on the fundamental diagrams, some studies have investigated the influence of VSL control systems on general measures of traffic flow such as lane use, speed variance, and shockwave mitigation. Under these considerations, the early work of Smulders (1990 and 1992) found that VSL reduced the fraction of small headways and more stable traffic flow. In doing so, throughput can be increased and congested conditions can be delayed. Likewise, Shi and Ziliaskopoulos (2002) used traffic flow and human behavior in the driving task to find that the benefits of VSL include improved safety, improved traffic flow, and more comfortable driving environments. The more recent research by Duret et al. (2012) studied the effects of VSL on lane flow distributions on a three-lane freeway in France. The results showed that VSL increased the use of the shoulder lane by decreasing the speed difference between the shoulder and passing lanes. Similarly, Nes et al. (2010) used driver simulation to analyze several VSL system designs. The study assessed driver compliance with each design as well as the

homogeneity of driving speeds. The authors concluded that dynamic speed control increased the homogeneity of driving speeds, with the best results coming from the advanced in-car system. In a like manner, Popov et al. (2008) developed a VSL control system to resolve shockwaves based on a distributed controller design technique, with each VSL sign having its own controller. Using METANET simulation (Messner and Papageorgiou, 1990), one study used traffic data in the immediate neighborhood of each VSL sign. The authors found that the proposed control method efficiently resolved shockwaves while reducing the total time spent by nearly 20%. The mitigation of shockwaves was also observed by Hegyi et al. (2005A).

Lastly, a few studies have analyzed the influence of VSL control on roadway capacity. Geistefeldt (2011) investigated the impact of VSL on freeway capacity in Germany. Using density and speed data, a five-minute capacity function was developed. The analysis compared the coefficient of variation of the predicted capacity under several speed control strategies. The author concluded that scenarios under VSL control had statistically significant lower coefficients of variation of the estimated capacity than those without VSL control. Thus, VSL control results in a lower risk of traffic breakdown in moderate volumes. In a similar evaluation of VSL control, Heydecker and Addison (2011) analyzed the relationship between speed and density for freeways under VSL control. Using one-minute aggregated data, a speed-density relationship was created using log-likelihood value comparisons. The study discovered that capacity increased when speed control was implemented. In a related study, Hegyi et al. (2005A) found that compared with the no-

VSL control case, VSL can restore outflows to capacity more quickly. In doing so, the total time spent can be decreased by up to 17.3%.

1.2.2. VSL in Recurrent Congestion

Due to the frequent and predictable occurrence of peak hour congestion in many of the world's urban networks, applications of VSL in recurrent congestion have become perhaps the most rigorously researched ATMS strategy. In fact, researchers from across the globe have investigated the potential for VSL control to improve mobility, safety, and environmental considerations. The remainder of this section summarizes those findings.

Similar to work zone studies, several evaluations of VSL in recurrent congestion have been carried out in simulated settings. Abdel-Aty et al. (2006) and Abdel-Aty et al. (2007) built on Abdel-Aty et al. (2005A) Abdel-Aty et al. (2005B). Using PARMAICS simulation software, the researchers showed that VSL could improve safety by using real-time data under medium- to high-speed traffic conditions. However, no significant improvement was found in the low speed scenarios. In a later study by Abdel-Aty et al. (2008), the use of homogeneous speed zones was introduced to determine the distance over which VSL would be implemented from a given target station. Using neural networks to classify crash and non-crash conditions, the overall risk change index was determined for rear-end and lane-change risks. The authors noted, "One of the most important factors in the crash risk models is the variance of speed between the station of interest and the nearest station upstream." The study found that VSL reduced both rear-end and lane-changing crashes under the 60% and 80% loading conditions. However, VSL did not have a significant

positive effect under congested conditions (90% loading). Next, Lee et al. (2004) used the real-time crash prediction model developed in Lee et al. (2002) and Lee et al. (2003) to evaluate the safety benefits of VSL on a Canadian freeway. Using the crash precursors of speed variation upstream of a target location, the spatial speed difference and the spatial lane volume difference, a model was calibrated to estimate the expected number of crashes on the study segment. The effect of VSL on crash frequency was tested under several VSL implementation strategies, conducted in a PARAMICS (Quadstone Limited, 2013) simulated environment. The study found that a lower threshold value for real-time crash potential for VSL activation produced a greater reduction in crash potential. In addition, the largest reduction in crash potential occurred in segments of high turbulence such as downstream of merging sections. Lastly, short VSL intervention periods were found to decrease the measures of safety as the speed limit changes too frequently. The authors also noted that while VSL improved safety, it often increased travel time. In 2008, Lee and Abdel-Aty used a driving simulator to assess the impact of speed change warning messages (via VMS) and VSL on driver speeds and compliance with posted speed limits. The study found that when the messages and VSL were displayed, speeds tended to be more uniform with less speed variation along the study segment. The authors concluded that such a VSL control system can not only improve safety but can improve the mobility of a freeway. In another simulated experiment, Kwon et al. (2011A) deployed a VSL control system on I-35 in the Twin Cities, Minnesota, to suppress the propagation of shockwaves in recurrent congestion. When a bottleneck is detected, the system is activated to reduce the speeds of approaching vehicles. The evaluation of the system was performed in a VISSIM-simulated

environment with 50% driver compliance to VSL. The results showed that the average maximum deceleration was reduced 15-48% paired with 3-15% increases in travel time. Likewise, the work by Grumert et al. (2013) used Simulation of Urban Mobility (SUMO) software (Krajzewicz, 2010) to assess the effect of a cooperative VSL system. The results showed that the cooperative VSL system harmonized traffic flow by increasing the proportion of large accelerations and decelerations. In doing so, emissions were also reduced under the cooperative VSL control system. Next, the team of Allaby et al. (2007) investigated the potential effects of VSL on safety and travel time using micro-simulation on a Canadian freeway. Safety was evaluated at several stations along the study corridor using the crash potential model developed by Lee et al. (2003) based on within-lane speed variation, spatial speed variation, and within-lane volume differences. Three scenarios were tested: peak, near-peak, and off-peak, using 100%, 90%, and 75%, respectively, of observed peak volumes. The analysis showed that the average safety benefit for all stations was 40% in peak conditions, 20% in near-peak conditions, and an 11% decrease in safety in off-peak conditions. The changes in travel times under peak, near-peak, and off-peak demand were 11%, 25%, and 1.3%, respectively. Moreover, Hegyi et al. (2005A) used model predictive control (MPC) developed by Hegyi (2004) to predict network evolution given current conditions in a METANET simulation framework. The MPC was used in a theoretical setting to activate an optimal coordinated VSL control system to resolve shock waves with the objective of improving the total travel time. Under safety constraints that limited the frequency of the speed limit change, the system showed a 17.3% reduction in total travel time. Finally, the Australian researchers Jiang et al. (2011) investigated VSL

under three scenarios: high flow, queuing, and adverse weather. This study analyzed the impact of VSL control algorithms used for the high flow and queuing scenarios in an Aimsun (TSS, 2013) simulation environment. The results showed that when ramp flows were small, VSL control improved travel time, speed deviation, fuel consumption, and emissions of CO₂. However, when ramp flows were high, measures of mobility increased under VSL control.

Field tests of VSL control in recurrent congestion are rarer than the previously discussed applications. Moreover, few road agencies in the United States have evaluated field-deployed VSL control. This realization indicates that observations from field tests of VSL in recurrent congestion are critical to understanding the potential of this ATMS method. Mirshahi et al. (2007) summarized ATMS strategies in Europe, some of which include VSL applications. Several European countries have field-deployed VSL systems, including the Netherlands, Finland, and Germany. These countries have found safety improvements from the use of VSL in congested and queuing environments on several major motorways. Similarly, Robinson (2000) provided a summary of domestic and international VSL applications. In the United States, VSL has been used to combat the ill effects of congestion in several states. In Michigan, advisory speed limits were tried on M-10 and I-94 in Michigan in the 1960s. However, the system was found to have little impact on vehicle speeds. From an international perspective, Germany installed an enforceable VSL system on the A3, A5, and A8 motorways to improve safety and reduce environmental impacts. The system has reduced the crash rate by 20-30 percent. The Netherlands has

experimented with a photo-enforced (during some periods) VSL system to relieve congestion. The system has been effective in reducing shockwaves associated with bottlenecks. In the UK, The Highway Agency (2007) reported on the costs and benefits of a mandatory VSL system installed on the M25 Controlled Motorway. The field-deployed VSL control system was evaluated in terms of several parameters, including safety, emissions, throughput, travel time, travel time reliability, and occurrence of flow breakdown, relative to the no-control case. The analysis found that injury crashes were reduced by 15% and the ratio of property damage only to injury crashes dropped by 20%. In terms of emissions, the VSL control system improved the measured emissions by 2-8%. The study found that VSL had little to no impact on common measures of mobility such as average travel time and travel time reliability. However, the VSL system improved overall traffic flow by reducing the occurrence of breakdown conditions and shockwave propagation. On the German Autobahn, Bertini and Bogenberger (2005) extended the research conducted by Bertini et al. (2004) by using fused data from multiple sources, including fixed freeway sensors, probe vehicles and GPS units. These data were used to identify the formation of recurrent bottlenecks. Next, the study analyzed the impact of the deployed VSL and VMS on driver behavior and bottleneck formation. The authors concluded that the VSL/VMS system was activated prior to and during bottleneck formation. In doing so, the system dampened the congested conditions. In a follow-up analysis, Bertini et al. (2006) built on Bertini et al. (2005) by examining recurring freeway bottlenecks on the German Autobahn. The research investigated the effect of VSL and traveler information systems on bottleneck formation by using fundamental diagrams. The

study found that when the system was activated, upstream speeds were reduced and flow into the bottleneck was reduced. As a result, the dense traffic continued to flow through the bottleneck. However, significant shockwave propagation was observed while the system was active. In yet another European application, Hegyi and Hoogendorn (2010) proposed and field tested the SPECIALIST VSL control algorithm on the Dutch A12 freeway. The study found that 80% of all detected shockwaves were resolved by using the algorithm. In doing so, on average the system saved 35 vehicle hours per resolved shockwave. However, the authors noted that approximately half of the activations were caused by jams other than shock waves. This efficiency issue was explained by the desire to detect shockwaves as early as possible, but it does not allow sufficient time to determine whether the shockwave is propagating upstream of the jam.

Further research by Hoogendoorn et al. (2013) assessed the impact of VSL on traffic operations, air quality, noise, and traffic safety on A20 in the Netherlands. The study found that VSL improved vehicle hours by 20% by increasing the capacity by 4% at the bottleneck area. Interestingly, VSL was found to increase emissions and noise levels. Furthermore, safety was evaluated using the speed differences between lanes, the speed standard deviation, the proportion of short headways, and the proportion of short-time to collision. The authors concluded that the assessment of the effects of VSL on safety was not possible due to the short analysis period. Similarly, Stoelhorst et al. (2011) analyzed VSL at four locations in the Netherlands, particularly the effects of VSL in terms of the travel time, air quality, noise, safety, and throughput. The results show that VSL

effectiveness depends on the conditions in which VSL is applied. The researchers concluded that while more studies need to be conducted, VSL has the potential to improve safety, mobility, and air quality.

In the United States, applications of VSL in recurrent congestion are limited. In fact, only two such studies have been conducted. The first such study was performed by Bham et al. (2010) on I-270/I-255 in St. Louis, Missouri. The objective of the study was to evaluate the effects of VSL in terms of safety and mobility. The study examined four segments along the control corridor and found that measures of mobility such as travel time increased under VSL control. In fact, travel times on these segments increased by 3.1%, 13.6%, -5.6%, and -19.1%. The authors concluded that these conflicting results may be caused by operational inefficiencies related to the traffic environment along each segment. To evaluate safety, a naïve and empirical Bayesian approach was used. While the results from each approach had slight differences, both found that VSL reduced the number of crashes, ranging from 4.5-8%. The second field study was conducted by Chang et al. (2011) and the related Pan et al. (2010). The study investigated the effects of an advisory VSL and a VMS traveler information system on travel time and throughput on a recurrently congested freeway near Baltimore, MD. The study evaluated the effect of three different ATM systems including VSL control only, a travel time display only, and VSL control paired with a travel time display. All three of these strategies showed an improvement in the average travel time of 7.5%, 5.1%, and 26.4%, respectively. These travel time improvements were paired with modest increases to the total throughput relative to the no

control case. Additionally, the study showed that VSL and VSL paired with a travel time display increased the average speeds in the control segment by 1.2 mph and 15.0 mph, respectively, thus reducing the spatial speed variance of the study section.

With many of the world's urban freeways being pushed to their capacity and limited resources to resolve the issue, traffic professionals have turned to ATMS and other demand management strategies to combat congestion. Among these strategies, VSL and ramp metering have been gaining international interest. As presented in this chapter, when VSL is properly applied, measures of safety and environmental impact are consistently improved. However, the evaluation of the effects of VSL on mobility was mixed. Some studies found that VSL increased travel times and total time spent, while others claimed that VSL improved these measures. It is worth reiterating that the aforementioned results come from both field and simulated studies where the objective and level of sophistication of VSL control algorithms used in these studies were not consistent. Therefore, it is reasonable to expect that a well-designed VSL control system can simultaneously improve measures of safety, mobility, and environmental impact.

In addition to the use of VSL alone, several studies have investigated the pairing of VSL with ramp metering. In contrast to VSL alone, many of these studies evaluated the integrated control strategy in terms of mobility. On this front, VSL paired with ramp metering consistently improved the total time spent. In fact, the mobility benefits from the pairing of VSL with ramp metering were greater than either independent strategy. Fewer studies focused on the safety benefits of VSL paired with ramp metering. However, the

results from these analyses show that the combination of VSL and ramp metering can reduce crash risk while improving travel times.

The tremendous contributions discussed above have established the potential of VSL and VSL paired with ramp metering to improve safety, mobility, and environmental considerations on recurrently congested freeways. However, most of these studies have evaluated these ATMS control methods at a single site. Thus, the development of a robust VSL and VSL paired with a ramp metering planning tool is needed. Such a tool would be useful for practitioners and traffic policy makers in deciding where and how to allocate limited resources for transportation improvement.

2. Research Objectives

2.1. Research Motivation

While the potential of VSL control and VSL paired with ramp metering to temper the negative effects of bottleneck formation is well documented in the literature, consistent guidelines on when, where, and how to implement VSL or VSL paired with ramp metering control are lacking. Such guidance should include details on the control algorithms for VSL control and VSL paired with ramp metering, including a method to safely create a speed transition zone from free-flow speeds down to the target control speed. Furthermore, these ground rules must give direction on the field deployment on both ATMS methods and assist in deciding when VSL control should be paired with ramp metering.

In addition, most of the previous work has focused on the evaluation of VSL control (or VSL paired with ramp metering) at a specific site suffering from the ill effects of a bottleneck. Although this methodology is useful for estimating the site-specific effects of VSL control, it does not directly assist decision makers with resource allocation. It is reasonable to assume that a large urban traffic agency will have several candidate sites for congestion mitigation efforts and will likely not have enough resources to implement an ATMS technology at all sites. Moreover, using traffic simulation to analyze VSL control at each candidate site would take tremendous time and effort from trained traffic simulation experts. Thus, a robust VSL planning model to predict the effects of VSL and VSL paired with ramp metering at candidate sites in terms of mobility, safety, and environmental impact would be useful for effective resource allocation. Such a model should use readily available candidate site-specific data as inputs. These inputs may include basic measures of traffic flow (i.e., V/C ratio, percent of trucks), road geometry (i.e., distance to adjacent interchanges) and assumptions/estimates on driver behavior (i.e., compliance with VSL).

2.2. Scope and Objectives

In light of the aforementioned VSL research needs, this section describes the specific objectives and associated key tasks of this research. The focus of this research was the application of VSL and VSL paired with ramp metering on recurrently congested freeways. However, many of the methodologies and contributions presented in this report may be relevant to other VSL applications. In any case, the goals of this research were to address some of the crucial issues in VSL research by establishing the following objectives:

1. Design a VSL control algorithm that allows for easy implementation of ramp metering control supplementation. Field deployment guidelines for such a VSL control system would also be developed.
2. Create a supplementary ramp metering control algorithm that includes equity considerations. Direction on the field implementation of this control system would be provided.
3. Develop a user friendly planning tool based on the expected changes in mobility, safety, and emissions resulting from VSL control or the combination of VSL and ramp metering.
4. Investigate the conditions that warrant VSL control or VSL paired with ramp metering. These results may also be useful for policy decision applications.

To accomplish the above mentioned objectives, this research was guided by the following keystone tasks:

Task 1: Present a thorough literature review of existing studies of VSL and VSL paired with ramp metering. This task will illustrate the various VSL deployment strategies, VSL control algorithms, commonly used evaluation methods, and results of VSL implementation in both field and simulated environments.

Task 2: Create several VSL control algorithms. The first set of algorithms should optimize VSL control in terms of minimizing travel time or speed variance while considering uncertainties such as driver behavior. The second general VSL design should allow for the easy supplementation of ramp metering. The VSL system must create a safe speed transition zone from free-flow conditions down to the desired control speed. Using real-time traffic data, the system can adapt to the evolution of the congestion. However, the activation, updating, and deactivation of the target control segment and control speed will be subject to safety constraints.

Task 3: Establish guidelines for the deployment of VSL control. These guidelines will establish the location of traffic detectors needed for accurate VSL control. In addition, the guidelines will include the placement of VSL signs and their respective spacing based on historical recurrent congestion patterns. The use of advanced warning signs to communicate when VSL control is in use will also be presented.

Task 4: Develop a ramp metering control algorithm designed to complement VSL control. The inputs of the ramp metering control system will share many of the same inputs as the VSL control system. As congestion builds from the bottleneck location, real-time equity considerations are implemented by coordinating upstream ramp meters.

Task 5: Establish guidelines for the deployment of supplemental ramp metering control based on the historical recurrent congestion patterns. These guidelines will establish which ramps to meter and the location of the associated detectors to be used as inputs into the control system logic.

Task 6: Using data from a VSL field deployment, calibrate a VSL simulation environment to be used as a basis for developing a robust data set to develop the planning module. Starting with the calibrated simulation, alter traffic flow parameters, road geometry features, and driver behavior variables to develop a diverse sample of possible VSL and VSL paired with ramp metering candidate sites. These simulations represent the “no control” (i.e., base) scenarios.

Task 7: For each no-control scenario exhibiting significant levels of congestion, implement the proposed VSL and VSL paired with ramp metering control strategies in the simulated environment. The effectiveness of each control system will be evaluated via changes in mobility, safety, and environmental impact relative to the no-control case. These results are used to develop predictive benefits models in the overall VSL planning tool.

Task 8: Create predictive models for the expected benefits of VSL and VSL paired with ramp metering. Relative changes in mobility, safety, and environmental impact are predicted from commonly known traffic parameters such as distance to adjacent interchanges, volume to capacity ratio (V/C ratio), and percentage of trucks.

Task 9: Discuss future research paths for the use of VSL and ramp metering in recurrent congestion conditions.

2.3. Organization of Report

This report consists of six sections. The following chapter presents the detailed methodology for the development of the VSL and ramp metering deployment guidelines. Next, the details of the optimized VSL control algorithms are presented, preceded by the VSL and the associated supplemental ramp metering control algorithms. The methodology section, then, describes the experiment design for developing the benefits models using a calibrated VISSIM simulation. The section concludes by discussing the statistical methods tested for predicting the safety and mobility benefits of VSL and VSL paired with ramp metering.

The findings section first presents the evaluation results of the optimized VSL algorithms. Next, the comparison of the benefits prediction models are presented. The findings section closes with a discussion on the best fitting models. Finally, conclusion and recommendations are presented in the final sections of this report.

3. Methodology

3.1. Optimal VSL Control

The proposed optimal VSL system consists of detectors, variable speed limit signs, and a central processing unit to execute control actions. The upstream detector in Figure 3-1 is used to capture the free-flow arrival rate, and a downstream detector is designed to record the discharging rate from the bottleneck. Also, additional detectors are placed at those on-ramps and off-ramps to record ramp arriving and departing flows. Several VSL signs along with detectors would be installed between the upstream and downstream detectors. In a field

application, those VSL signs shall dynamically update their displayed speed limit based on the computed optimal set of speeds and the specified criteria for VMS display.

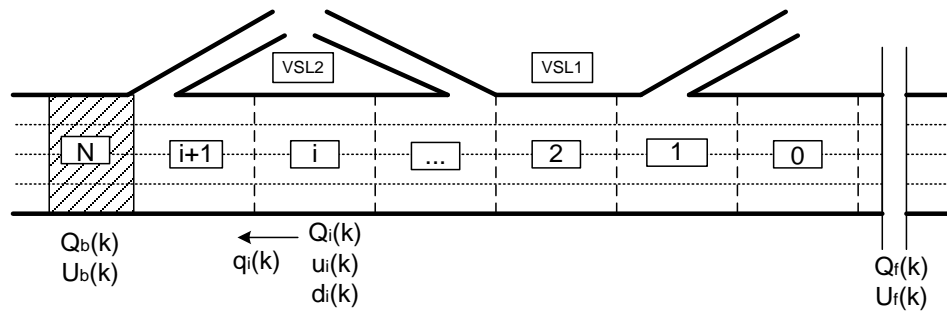


Figure 3-1. Typical Freeway Segments

Depending on the approaching volume, driver compliance rate, and the resulting congestion along the target freeway segment, a VSL system's central processing unit is responsible for producing the time-varying optimal speed limits. Note that for safety concerns and effective communications with drivers, all displayed speed limits are supposed to remain unchanged over the length of T^C seconds.

The operational structure of the proposed VSL control system includes the following two principal components:

- **Traffic State Estimation Model:** Given the detected upstream flow rate, the on-ramp and off-ramp flow rate, and the downstream discharging rate, the traffic flow model will function to estimate and predict the traffic state evolution in each freeway subsection;

- Optimization model: Based on the estimated conditions from the embedded traffic flow model, the system will execute the optimization model to predict the traffic state in the next prediction horizon and yield the set of optimal speed limits.

For the convenience of discussion, the control variables and parameters are listed below:

- Control time and subsection index:
 - ΔT : Unit time interval to update the traffic flow model;
 - T^P : Time interval for prediction horizon;
 - T^C : Time interval for control horizon;
 - k : Time interval index for the discrete traffic flow model.
- Network geometric and physical data:
 - ΔL : Length of each freeway segment;
 - n_i : Number of lanes in subsection i .
- Traffic states variables:
 - $q_i(k)$: Transition flow rate entering segment $(i+1)$ from segment i during interval k ;
 - $r_i(k)$: On-ramp flow rate entering segment i during interval k ;
 - $s_i(k)$: Off-ramp flow rate leaving segment i during interval k ;
 - $Q_i(k)$: Average flow rate in segment i during interval k ;
 - $d_i(k)$: Mean traffic density per lane in segment i during interval k ;
 - $u_i(k)$: Mean speed in segment i during interval k .
- Control variables, boundaries, and model parameters:
 - $v_i(k)$: Variable speed limit ratio in segment i during interval k ;

- d_j : Jam traffic density;
- u_j : Minimum mean speed;
- d_c : Critical traffic density;
- u_f : Free flow speed;
- q_{max} : Maximum flow per lane;
- γ : Congestion wave speed;
- δ : Maximum allowable difference for VSL change;
- α_i : Transition flow weight factor;
- v, τ, κ, a : Traffic state model parameters.

As shown in Figure 2, the target freeway segment is conceptually divided into N subsections with a unit length of ΔL . While dividing a freeway segment into subsections, the length of each subsection should be sufficiently long so that vehicles cannot pass one subsection during one time interval k . Moreover, each subsection is allowed to have at most one on-ramp and one off-ramp. For each subsection i , the mean density, $d_i(k)$, can be determined by the difference between the input and output flows as follows:

$$d_i(k+1) = d_i(k) + \frac{\Delta T}{\Delta L * n_i} [q_{i-1}(k) - q_i(k) + r_i(k) - s_i(k)] \quad (1)$$

For dynamically updating the average speed, $u_i(k)$, a well-developed equation proposed by Papageorgiou (1998) in his METANET model is adopted and shown as follows:

$$u_i(k+1) = u_i(k) + \frac{\Delta T}{\tau} \{V[d_i(k)] - u_i(k)\} + \frac{\Delta T}{\Delta l} u_i(k) [u_{i-1}(k) - u_i(k)] - \frac{v \cdot \Delta T}{\tau \cdot \Delta l} \frac{d_{i+1}(k) - d_i(k)}{d_i(k) + \kappa} \quad (2)$$

where $V[d_i(k)]$ is the static speed for segment i at time k with respect to the density $d_i(k)$:

$$V[d_i(k)] = u_f \cdot \exp\left[-\frac{1}{a} \left(\frac{d_i(k)}{d_c}\right)^a\right] \quad (3)$$

Also, the relationship between flow, density and speed is given by:

$$q_i(k) = d_i(k)u_i(k)n_i \quad (4)$$

Using the detected inflow rate from the upstream and on-ramp detectors, one can directly use Eq. 1-4 to estimate the traffic state evolution at the target freeway segment.

Based on the estimated traffic state, one can further implement the traffic flow model (Eq. 1-4) to predict the traffic state within the next specified horizon with respect to different speed limits. Then, the one with the best objective output can be selected for implantation. Hence, the first step of the optimization model is to select a proper control objective function.

As the primary focus of VSL is to increase traffic flow speed and its stability, this study first adopts the following objective of minimizing total travel time over the controlled segment:

$$\min \sum_k \sum_i n_i d_i(k) \Delta T \quad (5)$$

Note that depending on the response of drivers to the displayed speeds, the embedded macroscopic traffic flow models and the above objective function may not fully capture the complex traffic dynamics and yield the true optimal results.

As reported in the literature [Steel et al. (2005), Ulfarsson et al. (2005), and Anund et al. (2009)], a proper VSL control can help smooth speed transition and consequently reduce the number of vehicle stops and shockwave impact on the traffic conditions [Chang et al. (2011)]. Hence, this study has further explored the following objective function of minimizing the speed variance along the target freeway for a VSL control:

$$\min \sum_k \sum_i (u_i(k) - u_{ave})^2 \quad (6)$$

where u_{ave} is the average speed of the target freeway stretch, and is given as follows:

$$u_{ave} = \frac{\sum_k \sum_i u_i(k)}{(T^c / \Delta T) \cdot N} \quad (7)$$

To implement the optimization model and select the proper control speed limit for the projected control period, one shall place the following additional constraints.

For each subsection i , its mean speed shall not exceed the displayed speed limit:

$$\begin{cases} u_j \leq u_i(k) \leq u_f, & \text{segment } i \text{ without VSL control;} \\ u_j \leq u_i(k) \leq u_f v_i(k), & \text{segment } i \text{ with VSL control.} \end{cases} \quad (8)$$

where

$$0 < v_i(k) \leq 1 \quad (9)$$

One shall also set the density boundaries to reflect the jam density constraint as follows:

$$0 \leq d_i(k) \leq d_j \quad (10)$$

Also, for safety concerns, the speed variation between consecutive intervals shall be set within the following boundaries.

$$-\delta \leq u_i^f v_i(k) - u_i^f v_i(k-1) \leq \delta \quad (11)$$

where δ is the maximum allowable difference between two successive speeds displayed on VMS.

In reality, the freeway congestion may be caused by many factors aside from an increase in traffic demand. For example, traffic weavings can result in the formation of bottlenecks. Therefore, due to the limitation of macroscopic traffic flow models, this study has further adopted the Kalman Filter, which has proven to be effective for updating model parameters in real-time operations [Wang and Papageorgiou (2005)], to improve the estimation accuracy. The Kalman Filter is an optimal state estimator applied to a dynamic system that involves random noise and includes a limited amount of noisy real-time measurements. The correction and update process of a typical Kalman Filter process is summarized in Figure 3-2.

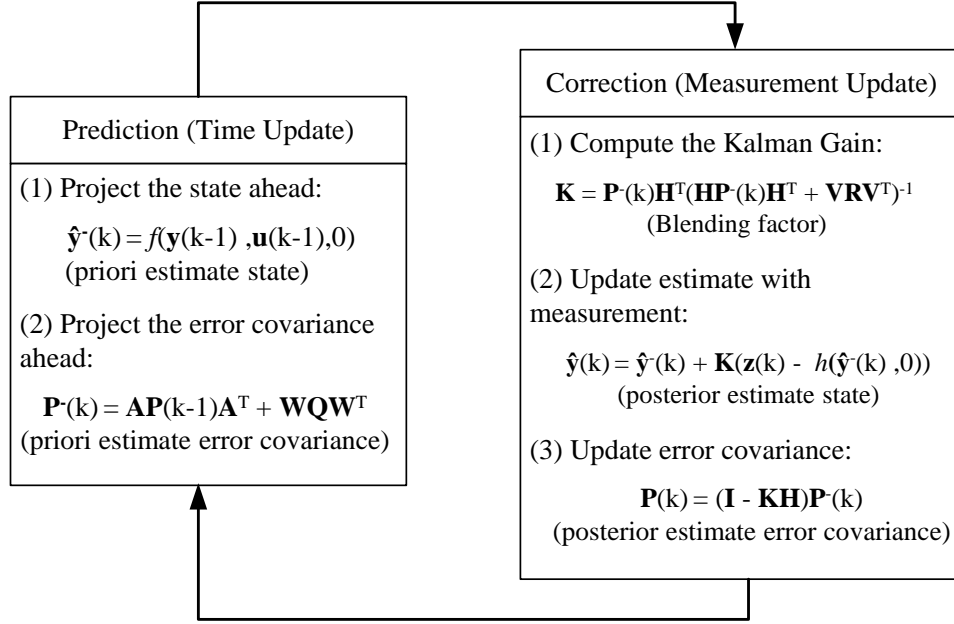


Figure 3-2: An Illustration of Kalman Filter Correction and Update Process

where $\mathbf{y}(k)$ is the estimated traffic state vector:

$$\mathbf{y}(k) = [q_1(k) \ u_1(k) \ q_2(k) \ u_2(k) \ \cdots \ q_N(k) \ u_N(k)]^T \quad (12)$$

And $\mathbf{u}(k)$ is the system input:

$$\mathbf{u}(k) = [q_0(k) \ v_0(k) \ q_{N+1}(k) \ v_{N+1}(k) \ r_1(k) \ \cdots \ r_N(k) \ s_1(k) \ \cdots \ s_N(k)]^T \quad (13)$$

Also, $f(\cdot)$ represents the traffic flow model shown by equations 1-4, and $\mathbf{z}(k)$ denotes the vector of measurements. In a typical VSL system shown in Figure 3-1, it collects three types of measurements in real time, including freeway flow rate, freeway speed, and on-ramp flow rate.

The measurements $\mathbf{z}(k)$ has the following relation with $\mathbf{x}(k)$:

$$\mathbf{z}(k) = h(\mathbf{y}(k), \mathbf{v}(k)) \quad (14)$$

where $\mathbf{v}(k)$ is the measurement error.

Four important matrices involved in the computations are shown below:

\mathbf{A} is the Jacobian matrix of partial derivatives of function $f(\cdot)$ with respect to \mathbf{x} :

$$\mathbf{A}_{[i,j]} = \frac{\partial f_{[i]}}{\partial y_{[j]}}(\mathbf{y}(k-1), \mathbf{u}(k-1), 0) \quad (15)$$

\mathbf{W} is the Jacobian matrix of partial derivatives of function $f(\cdot)$ with respect to process noise

\mathbf{w} :

$$\mathbf{W}_{[i,j]} = \frac{\partial f_{[i]}}{\partial w_{[j]}}(\mathbf{y}(k-1), \mathbf{u}(k-1), 0) \quad (16)$$

\mathbf{H} is the Jacobian matrix of partial derivatives of function $h(\cdot)$ with respect to \mathbf{x} :

$$\mathbf{H}_{[i,j]} = \frac{\partial h_{[i]}}{\partial y_{[j]}}(\mathbf{y}(k), \mathbf{v}(k)) \quad (17)$$

\mathbf{V} is the Jacobian matrix of partial derivatives of function $h(\cdot)$ with respect to measurement

noise \mathbf{v} :

$$\mathbf{V}_{[i,j]} = \frac{\partial h_{[i]}}{\partial v_{[j]}}(\mathbf{y}(k), \mathbf{v}(k)) \quad (18)$$

By using the Kalman Filter, the estimated traffic state can be constantly updated based on the detector data, and the new optimal speed limits can then be generated with the proposed

optimization model. Assuming that the VSL's control horizon and prediction horizon are set to be 5 minutes and the detector data are updated at an interval of every minute, then each control interval will have five sets of estimated optimal speed limits prior to its implementation time, as shown in Figure 3-3.

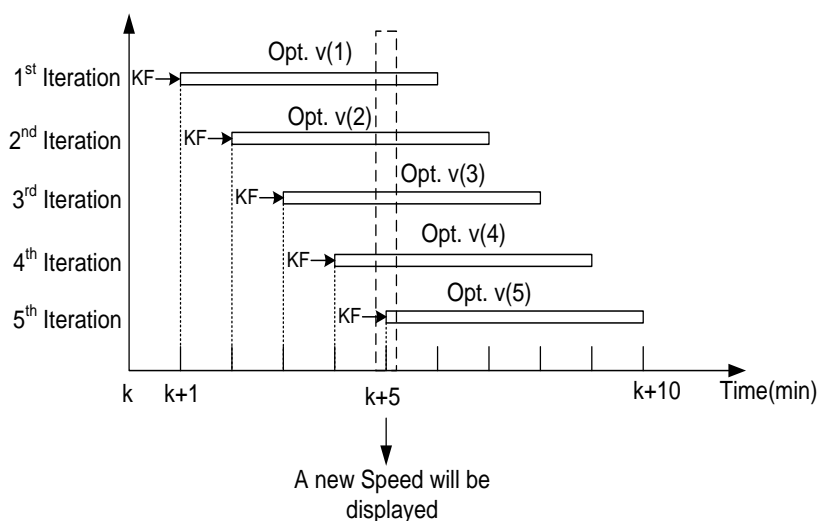


Figure 3-3: Example of the VSL Control Strategy

Given the set of computed optimal speed limits for the same horizon, $\{v(1), v(2), \dots, v(n)\}$, one can determine the speed limits to be displayed based on the following procedure:

- 1) Define a counter M to identify the moving direction of the speed limit, and then denote v^t as the displayed speed limit of the current horizon, where M is updated by the following expression:

$$M = \begin{cases} M + 1, & \text{if } v(i) > v^t \\ M, & \text{if } v(i) = v^t, \quad i=1,2,\dots,n; \\ M - 1, & \text{if } v(i) < v^t \end{cases} \quad (19)$$

2) The new displayed speed limit for the next horizon will be readjusted with the predetermined increment Δ , based on the value of M :

$$v^{t+1} = \begin{cases} v^t + \Delta, & \text{if } M > 0 \\ v^t, & \text{if } M = 0 \\ v^t - \Delta, & \text{if } M < 0 \end{cases} \quad (20)$$

The operational flow chart of the VSL control system is presented in Figure 3-4.

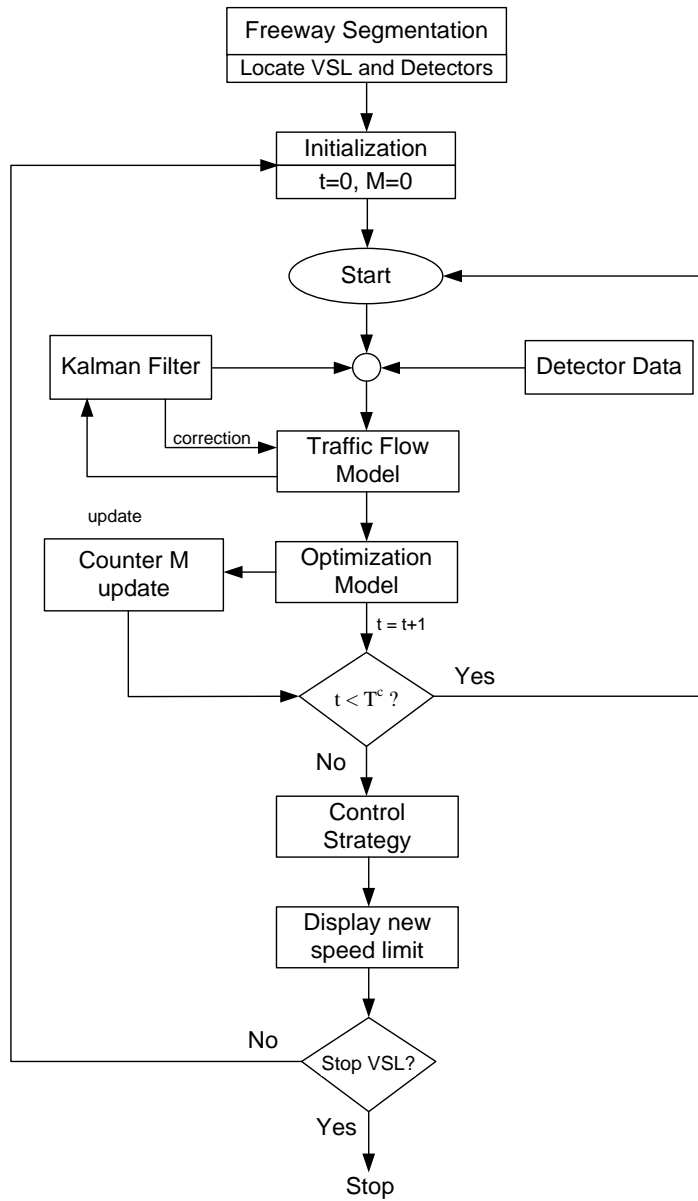


Figure 3-4. Flow Chart of the Enhanced Proactive Model VSL Control System

3.2. VSL Control with Ramp Metering

3.2.1. General VSL Control Logic

The control parameters of the proposed VSL system are based on examining the flow into and out of the congested segment, constrained by spatial and temporal speed changes. Recognizing that the severity and extent of congestion are dynamic, the overall congested segment is further divided into sub-segments. Each sub-segment uses detectors at each entrance/exit point of the sub-segment to monitor inflow/outflow. The details of defining the sub-segments as well as the associated detector locations are discussed in detail in the deployment guidelines section of this chapter. In any case, the advantage of the sub-segment control methodology is twofold. First, as the system monitors traffic conditions in each sub-segment, determinations on the severity and extent of the congestion can be made and used to define the dynamic control strategy. For example, if the farthest downstream sub-segment becomes entirely queued, then mainline inflow control will no longer be possible. Therefore, the system should seek to control inflow into the immediate upstream segment. Second, the sub-segment control methodology allows for easy supplementation of ramp metering control. By defining the congested sub-segments, the appropriate supplemental ramp metering control strategy can be executed.

Note that upon system activation, the 10 mph step down to the target control speed strategy will be executed. In doing so, the speeds at the upstream detectors may meet the criteria to control inflow into upstream sub-segments when in fact it is the control system that has created this speed drop, not the congestion. To prevent this scenario from occurring, it is

critical to determine which sub-segment is the target control sub-segment. Assuming that the congestion builds from the bottleneck location, the most downstream sub-segment exhibiting a minimum 10 mph speed drop from the mainline inflow detector to the mainline outflow detector will be selected as the target control sub-segment. This definition of the target control sub-segment not only prevents the artificial activation of flow control for upstream sub-segments; it also allows for the VSL control system to shift to controlling flow into the upstream sub-segments if the downstream sub-segment(s) become entirely queued.

To effectively control the inflow of vehicles under VSL control, the structure of the proposed algorithm is based on three primary components:

1. System activation component: This component decides when to turn on the VSL control system based on threshold densities and spatial speed differences. Once activated, the associated infrastructure including VSL signs and advanced warning systems, will be turned on to communicate the control speeds to motorists.
2. VSL control speed updating component: Upon system activation, this component determines the extent and severity of the congested segment. This information is used to define the target control sub-segment and its respective control speed. If required, additional upstream VSL signs will be used to safely step down speeds to the target control speed. Additionally, this component considers driver adherence to the posted VSL by comparing the target speed to the observed speed in a feedback loop.
3. System de-activation component: As congestion dissipates and the bottleneck dissolves, VSL will no longer be needed. This component controls the systematic de-activation of VSL to safely return the control segment back to the posted speed limit.

Each component uses real-time traffic data as inputs into the functions for VSL control logic. The overall operational flow chart of the VSL control system is presented in Figure 3-5, where the primary components are in bold text. The details of each component are presented in the following sections.

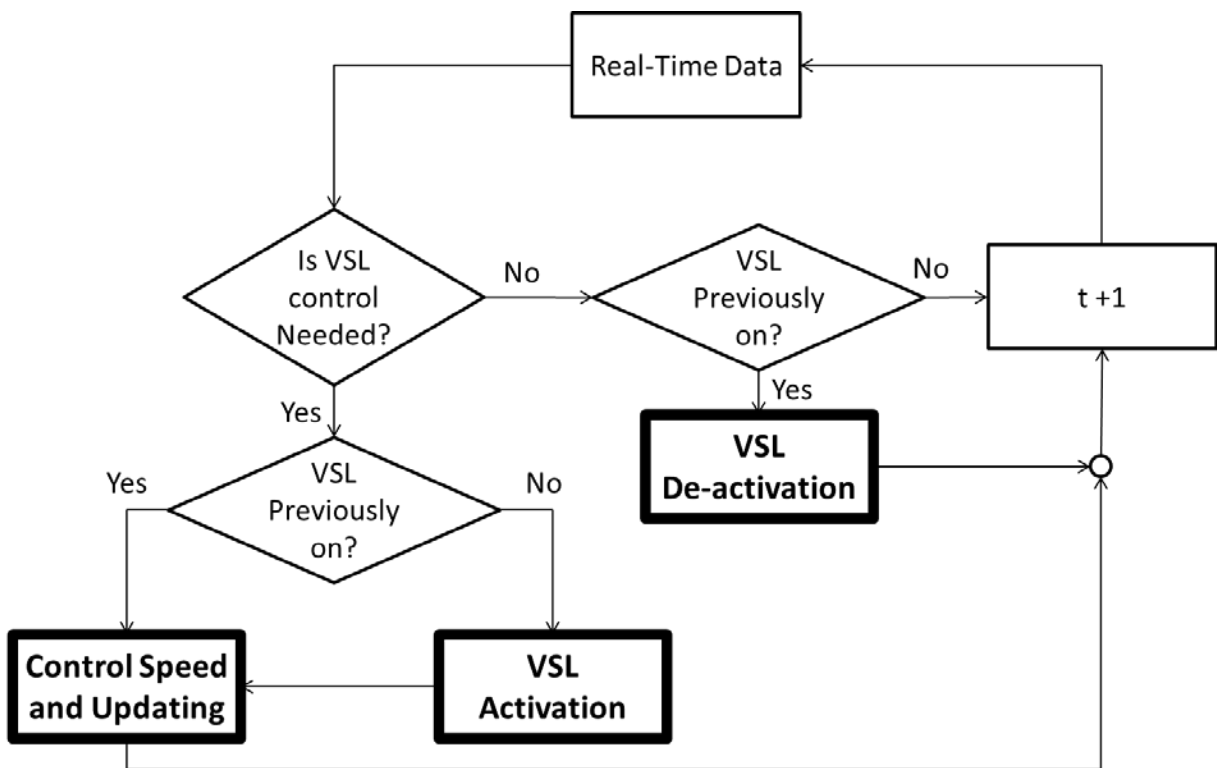


Figure 3-5: VSL Control Operational Flow Chart

3.2.2. VSL System Activation

The determination of the criteria for system activation is a crucial issue in the design of a VSL control system. If the system is activated too soon, drivers will not see the need to obey the displayed speeds. On the other hand, if the system is activated too late then the required

inflow control may be beyond the limits of the VSL control system. In either scenario, drivers will have negative perceptions of the system, which may result in diminished benefits in terms of congestion mitigation.

The activation of the proposed VSL algorithm and determination of the control sub-segment is based on observed speed differences between adjacent mainline detectors. In the pre-activation phase, traffic is monitored using 1-minute aggregated data. Specifically, if the downstream detector in a mainstream detector pair drops 10 mph or more below the speed at the upstream detector, then the VSL system will be activated.

Once activated, all VSL signs and the advanced warning signs will be turned on and the system will be updated every five minutes to avoid too frequent changing of the displayed VSL speeds. Those VSL signs not needed in the activation interval will simply display the original posted speed limit. This activation strategy is designed to reduce driver confusion as vehicles enter the control segment. If the unneeded VSL signs are not turned on, drivers may perceive that the system is not working or that the signs are malfunctioning. The next section describes the target control speed calculation used for selecting the VSL display speeds at each update interval.

3.2.3. VSL System Activation

Upon system activation, the control system must determine the target control sub-segment and the appropriate target control speed. This initial determination is performed using the 1-minute aggregate data that activated the VSL control system. All subsequent target control speeds are based on 5-minute aggregated data from the target control sub-segment. In either

case, the target control speed is derived from the fundamental equation using the observed flows into and out of the target control sub-segment and its length. Since the system is constrained to speed updates of 10 mph increments from the original speed limit, the control speed is rounded to the nearest 10 mph as follows:

$$v_c^i(t) = \text{round} \left[\frac{q_{down}^i(t-1)}{k_i(t)}, -1 \right] \quad (21)$$

and

$$k_i(t) = k_i(t-1) + \frac{q_{in}^i(t-1) - q_{out}^i(t-1)}{L_i} \quad (22)$$

where

$v_c^i(t)$ = target control speed into sub-segment i for time interval t (mph)

$q_{down}^i(t-1)$ = total mainline outflow out of sub-segment i in the previous time interval

$q_{in}^i(t-1)$ = total inflow into sub-segment i in the previous time interval

$k_i(t)$ = density of sub-segment i at the start of time interval t

L_i = Length of sub-segment I (miles)

Keep in mind that the control speed can only change by ± 10 mph in a consecutive update interval. Thus if the control speed is calculated to be ± 20 mph or more, the system will select a ± 10 -mph change and reevaluate the required target control speed at the next 5-minute update interval. Thus:

$$v_c^i(t) = \begin{cases} v_c^i(t-1), & \text{if } v_c^i(t) - v_c^i(t-1) = 0 \\ v_c^i(t-1) - 10, & \text{if } v_c^i(t) - v_c^i(t-1) \leq -10 \\ v_c^i(t-1) + 10, & \text{if } v_c^i(t) - v_c^i(t-1) \geq 10 \end{cases} \quad (23)$$

where

$v_c^i(t)$ = target control speed for the current time interval t (mph)

$v_c^i(t-1)$ = target control speed for the previous time interval $t-1$ (mph)

Once the target control speed is defined, the display speeds for the other VSL signs can be determined using the 10-mph step-down strategy. If the target control speed is more than 20 mph below the original speed limit, then multiple signs will be needed to create a safe speed transition zone.

If and when congestion continues to build under VSL control, the initial target control sub-segment may become entirely queued. As a result, the speeds between the downstream and upstream detectors may become less than 10 mph. However, the speeds at both the downstream and upstream detectors will be 10 mph or more below the original speed limit. In this situation, the proposed VSL control system will shift to controlling the inflow speeds into the upstream sub-segment. The target control sub-segment can be determined by:

$$S_{Control} = \begin{cases} i, & \text{if } v_{up}^i - v_{down}^i \geq 10 \\ i + 1, & \text{if } v_{up}^i - v_{down}^i < 10 \text{ and } v_{up}^i \leq PSL - 10 \\ i + 2, & \text{if } v_{up}^{i+1} - v_{down}^{i+1} < 10 \text{ and } v_{up}^{i+1} \leq PSL - 10 \\ \vdots & \\ I, & \text{if } v_{up}^{I-1} - v_{down}^{I-1} < 10 \text{ and } v_{up}^{I-1} \leq PSL - 10 \end{cases} \quad (24)$$

where

$S_{Control}$ = target control sub-segment

i = bottleneck sub-segment identifier

I = total number of sub-segments

v_{up}^i = 5 minute average speed at the upstream boundary of sub-segment i (mph)

v_{down}^i = 5 minute average speed at the downstream boundary of sub-segment I (mph)

PSL = original posted speed limit (mph)

The target control speed calculation is performed using the data from the new (upstream) target control sub-segment. The unshared VSL signs for controlling the now queued segment will display the smaller of the detected speeds with the queued sub-segment or the upstream target control speed.

Eventually, the peak period demand will diffuse and the need for inflow control will be reduced until it is no longer needed. If the entire VSL control system were simultaneously shut off, a secondary bottleneck might be created from the sudden flux of vehicle inflow. Thus, the de-activation component is designed to handle the transition from congestion back to stable traffic flow. The operation of the de-activation component is similar to the target control speed and updating component, but is designed to shut down the VSL control system by systematically returning speeds back to the original posted speed limit.

The control system de-activation component uses real-time traffic conditions within the target control segment to determine when to start the decommissioning of VSL control. It is worth noting that the maximum severity of the speed drop within a given sub-segment is a function of the distance from the bottleneck. Thus, farther upstream sub-segments will typically return to free-flow conditions earlier than downstream sub-segments. However, shockwave theory explains that upstream conditions cannot improve until the downstream bottleneck begins to dissolve. Therefore, as the conditions at the bottleneck improve, the associated queues will dissipate and previously required upstream VSL signs will no longer be needed.

As designed, the updating component of the control system can effectively adjust to improving conditions. However, eventually the target control sub-segment will need to shift back toward the bottleneck as conditions improve. Thus, the primary function of the de-activation component is to provide this shift and to update the unneeded VSL signs to display the original posted speed limit. The de-activation process begins at the farthest

upstream target control sub-segment when speeds begin to recover. Once the speeds at the downstream boundary of the most upstream sub-segment are within 10 mph of the posted speed limit, flows into this sub-segment will no longer need to be regulated. Thus, the control system will shift the target control sub-segment to the next most upstream sub-segment as follows:

$$S_{Control} = \begin{cases} I, & \text{if } v_{up}^I - v_{down}^I \geq 10 \\ I - 1, & \text{if } v_{up}^I - v_{down}^I < 10 \text{ and } v_{down}^I \geq PSL - 10 \\ I - 2, & \text{if } v_{up}^{I-1} - v_{down}^{I-1} < 10 \text{ and } v_{down}^{I-1} \geq PSL - 10 \\ \vdots & \\ i, & \text{if } v_{up}^{i+1} - v_{down}^{i+1} < 10 \text{ and } v_{down}^{i+1} \geq PSL - 10 \\ \text{System Off}, & \text{if } v_{up}^i - v_{down}^i < 10 \text{ and } v_{down}^i \geq PSL - 10 \end{cases} \quad (25)$$

Here, the variable definitions are identical to those in equation 4. As upstream signs become unneeded to control inflow, they will return back to displaying the original speed limit under the same identical constraints in the updating component. That is, each sign can only change by ± 10 mph for each update interval and the maximum speed change between consecutive signs is 10 mph. This process is repeated until the bottleneck sub-segment returns to uncongested conditions. At this point, the VSL control will terminate by turning off all VSL signs and advanced warning messages.

3.2.4. Supplemental Ramp Metering Control Algorithm

The basis of any ramp metering strategy is to govern inflow into a congested segment by controlling the vehicle entrance rate from on-ramps. As described in the literature review section,

the varying objectives and levels of control algorithm sophistication have resulted in several methods to activate the system and to estimate the appropriate ramp metering rate.

In the proposed ramp metering control algorithm, ramp metering is activated once a critical cumulative difference in inflow and outflow is detected. This critical difference in inflow and outflow is based on the critical density established from field data on the proposed control segment. The associated ramp metering rate is determined by calculating the difference between observed cumulative differences in inflow and outflow and the critical value. If the calculated ramp metering rate is below the pre-determined minimum ramp metering rate, the immediate upstream ramp meter may be activated for supplementary inflow control (if an upstream meter exists). In such instances, metering equity is considered based on real-time demand patterns on each respective on-ramp.

As will be presented in the following sections, the overall ramp metering control logic can be segregated into four primary components:

1. Activation Component - Responsible for determining when ramp metering should be turned on for a given on-ramp based on cumulative differences in observed inflow and outflow into a given sub-segment within the pre-defined congestion segment.
2. Upstream Ramp Supplementation Component - When the calculated ramp metering rate exceeds the limits of a given ramp meter, the immediate upstream ramp meter may be activated for additional inflow control.
3. Ramp Queue Override Component - Before ramp metering activation and at each ramp metering rate update, the queue on the associated ramp is checked. If the max queue is

detected, appropriate actions are taken to reduce the queue within the constraints of the control algorithm.

4. De-activation Component - As congestion dissipates, ramp metering for inflow control is no longer needed. This component defines the criteria for shutting down ramp metering control.

The general ramp metering control algorithm flow chart can be visualized in Figure 3-6. The details of the ramp metering control algorithm are presented in the following sections. The following variable definitions for the figure are provided:

- t_r = time interval index (30 seconds)
- T = total number of time intervals in analysis period
- I = total number of metered ramps
- R_i = ramp i
- RMR_i = ramp metering rate for ramp i
- RMR_i^* = upstream supplemental ramp metering rate
- RM_i = metering activation switch for ramp i
- R_{iOFF} = metering deactivation counter (set to 5)
- QC_i^{On} = ramp queue deactivation counter QC_i = Ramp queue over-ride switch
- $b_i(t)$ = cumulative difference between inflow and outflow on segment i at time t

- X_i = cumulative difference in inflow and outflow threshold for sub-segment i
- Y_{OFF} = ramp metering deactivation threshold
- Z_{OFF} = ramp queue deactivation threshold (set to 2)

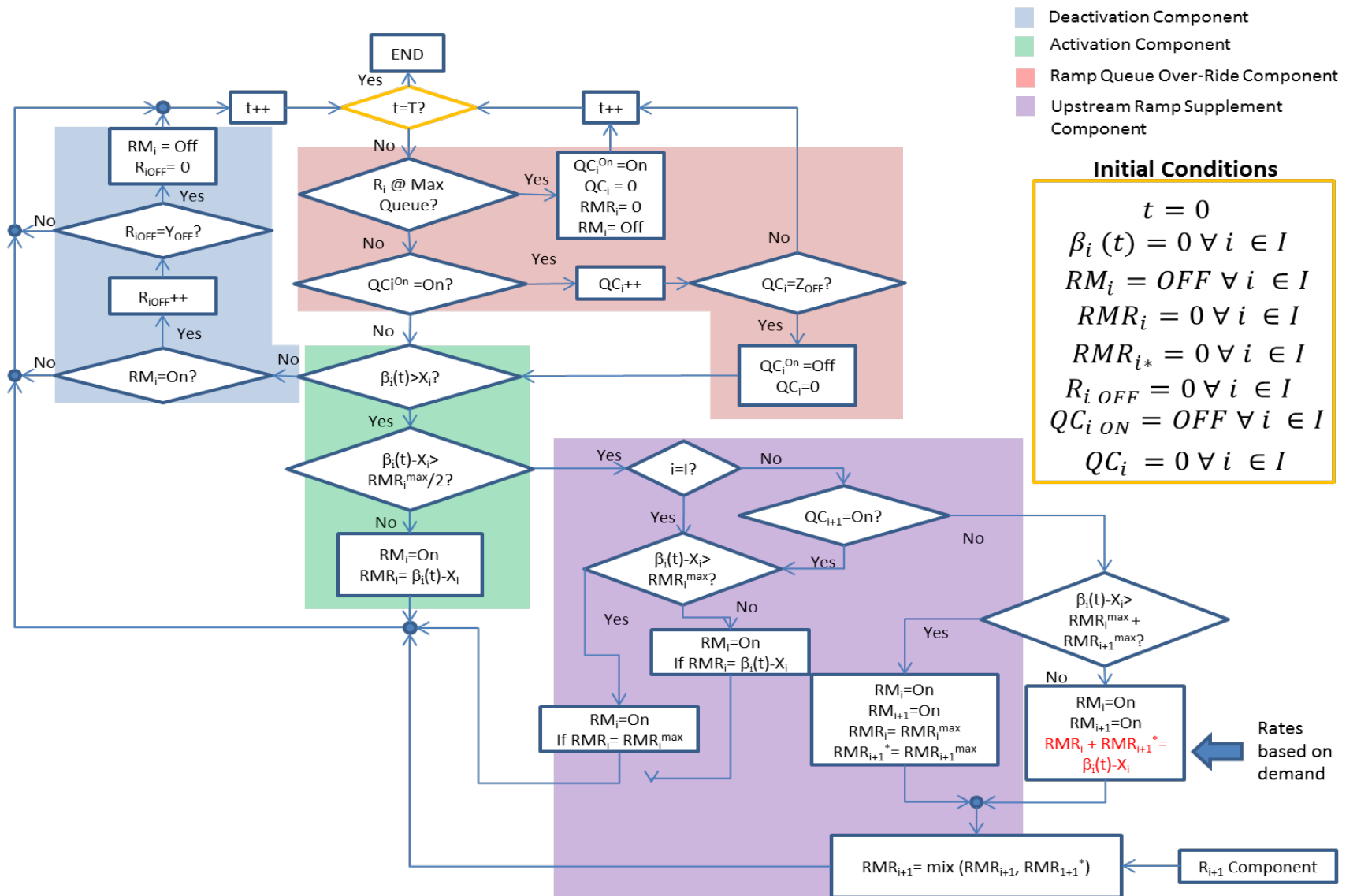


Figure 3-6: Ramp Metering Control Flow Chart

3.2.5. Ramp Metering Activation

As described in the ramp metering deployment guideline section, several detectors are used to monitor real-time traffic flows into and out of each sub-segment. Total inflow is simply the sum of all entrance points into the sub-segment. In a similar fashion, total outflow from a sub-segment can be computed. As congestion builds, the cumulative difference in inflow and outflow will build up to a critical value. This critical difference in inflow and outflow can be derived from the flow-density relationship of the target sub-segment. The objective of the proposed ramp metering control is to intervene as conditions approach the critical density. In doing so, the inflow will be throttled so as to keep the sub-segment in the stable flow regime of the flow-density diagram. Thus, applying a conservative estimate of the critical density will meet this need. With knowledge of the length of each sub-segment, the critical density can be converted into a critical cumulative difference in inflow and outflow using the following equation:

$$k_i^{crit} * L_i = X_i^{crit} \quad (26)$$

where

k_i^{crit} = critical density on sub-segment i

L_i = length of sub-segment i

X_i = critical cumulative difference in inflow-outflow on sub-segment i

In the proposed ramp metering control algorithm, these inflow and outflow data are sent to the system controller for ramp metering decisions every 30 seconds. Therefore, the cumulative difference in inflow – outflow can be computed as:

$$\beta_i(t) = \beta_i(t - 1) + q_i^{in}(t) - q_i^{out}(t) \quad (27)$$

where

$t = 30$ second time interval step

$\beta_i(t)$ = observed cumulative difference in inflow-outflow on sub-segment i at time t

$q_i^{in}(t)$ = total inflow into sub-segment i during time interval t

$q_i^{out}(t)$ = total inflow out of sub-segment i during time interval t

A few subtleties regarding equation 2 warrant further discussion. First, equation 27 assumes the sub-segment empty during activation. If this condition cannot be satisfied in practice, then an estimate of vehicles with the sub-segment at activation will be needed. For instance, if the system is activated when 10 cars are within the boundaries of the target sub-segment, and assuming all 10 cars exit the downstream mainline boundary, then the system will have a 10-car outflow bias. Similarly, during non-congested conditions some vehicles may enter the sub-segment at the end of the time interval and may not have sufficient time to traverse the entire sub-segment before the end of the time interval step. This condition would obviously bias the inflow count for that time interval. However, those vehicles that were counted as inflow for one time interval will be counted as outflow during the next time interval, assuming the sub-segment can be traversed in a single time interval. Thus, the cumulative difference in inflow and outflow will naturally stay below the critical value in non-congested conditions.

Finally, at the end of each time interval the result of equation 2 is compared to the pre-defined critical cumulative difference in inflow and outflow for each sub-segment. Once the

cumulative difference in inflow and outflow exceeds the threshold, the ramp meter (or meters if the sub-segment has multiple on ramps) will be turned on for that sub-segment. This process can be visualized in Figure 3-7. If a sub-segment with multiple on-ramps displays a cumulative inflow-outflow above the threshold value, then all ramps may be turned. The associated ramp metering rates will incorporate equity considerations based on recent demand patterns.

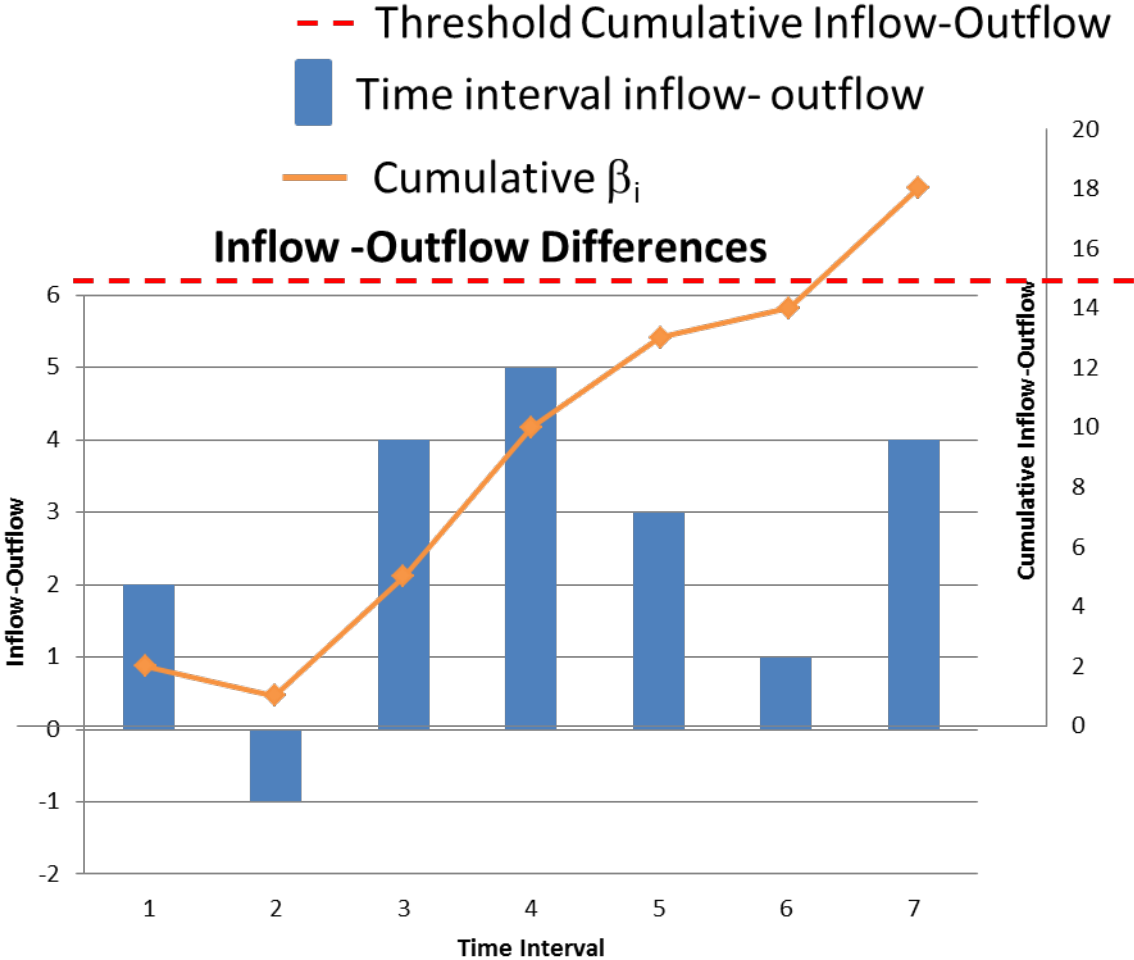


Figure 3-7: Ramp Metering Activation

As shown in Figure 3-7, the ramp meter would be activated at the start of time interval 8. The following section will describe how the metering rates are calculated.

3.2.6. Ramp Queue Override and Ramp Metering Rate

Recognizing that ramp metering seeks to mitigate congestion by controlling inflow from nearby on-ramps, the potential for causing excessive delay to the ramp vehicles exists. In addition, long ramp queues can spill back onto the connecting roads, causing widespread congested conditions. To avoid this scenario, most ramp metering algorithms employ a maximum ramp queue constraint.

While several queue detection/estimation methods exist, the proposed control algorithm uses the observed difference in ramp inflow and outflow to determine the queue length (number of vehicles) at the start of each time interval. This calculation is performed as follows:

$$\theta_{ramp\ i}(t) = \theta_{ramp\ i}(t - 1) + q_{ramp\ i}^{in}(t) - q_{ramp\ i}^{out}(t) \quad (28)$$

where

$\theta_{ramp\ i}(t)$ = queue on ramp i at the end of time interval t (number of vehicles)

$\theta_{ramp\ i}(t-1)$ = queue on ramp i at the end of the previous time interval (number of vehicles)

$q_{ramp\ i}^{in}(t)$ = inflow onto ramp i during time interval t

$q_{ramp\ i}^{out}(t)$ = outflow from ramp i during time interval t

Having established the calculation for ramp queues, the maximum allowable queue lengths need to be defined. As done by Papageorgiou (2002), this study assumes a maximum acceptable on-ramp queue length of 20 vehicles. For freeway-to-freeway interchanges, the

maximum acceptable queue length is 90 vehicles. Recognizing that ramp metering is usually installed prior to ramp and interchange design and construction, these acceptable lengths should be compared with the existing physical storage capacity of the on-ramp or interchange ramp being considered for ramp metering installation. This calculation requires an estimate of the average vehicle length. If possible, field data should be used to estimate this parameter. Otherwise an assumed vehicle length may be used. In the case where the on-ramp or interchange does not provide sufficient storage to meet the aforementioned acceptable queue lengths, an alternative method is suggested. This method is based on the findings of Hasan (1999), who found that on-ramp queue detectors placed at 75 percent of the physical ramp length outperformed detectors at 100 and 62.5 percent of the ramp length. In this application, the maximum acceptable queue length is defined to be 75 percent of the ramp length, given an average vehicle length. With this consideration in mind, the maximum acceptable queue length for an on-ramp is defined as:

$$q_{ramp\ i}^{max} = \min \left[20 \text{ vehicles}, \frac{0.75L_{ramp\ i}}{VL} \right] \quad (29)$$

where

$q_{ramp\ i}^{max}$ = maximum acceptable queue on ramp i (number of vehicles)

$L_{ramp\ i}$ = length of ramp i (ft)

VL = average vehicle length (ft)

In a similar fashion, the maximum acceptable queue length for a freeway-to-freeway interchange ramp is:

$$\theta_{ramp\ i}^{max} = \min \left[90 \text{ vehicles}, \frac{0.75L_{ramp\ i}}{\bar{V}L} \right] \quad (30)$$

where

$q_{ramp\ i}^{max}$ = maximum acceptable queue on ramp i (number of vehicles)

$L_{ramp\ i}$ = length of ramp i (ft)

$\bar{V}L$ = average vehicle length (ft)

The maximum queue constraint is checked before ramp metering is activated and each time the metering rate is updated. If a given ramp that had not been previously activated shows a cumulative sub-segment inflow-outflow above the threshold, the ramp queue will be checked before that ramp is turned on. If the queue exceeds the maximum allowable queue, then the ramp will remain de-activated and that ramp becomes ineligible for ramp metering activation until the observed queue is below the maximum queue for two consecutive update intervals. On the other hand, if the ramp meter is already activated and the queue exceeds the maximum queue, then the ramp metering rate is set to the maximum rate. The maximum rate will be applied until the observed queue is below the maximum queue for two consecutive update intervals.

3.2.7. Upstream Ramp Metering Supplementation

When the calculated ramp metering rate is below half of the maximum ramp metering rate for the target sub-segment, the immediate upstream ramp meter will be called on for inflow control supplementation if it is available. Since the sub-section upstream boundary was

defined to be at the merge area of the upstream sub-section on-ramp, the effect of upstream ramp metering supplementation will be realized in the target control interval. In this study, only the immediate upstream ramp meter can be used for supplementation.

In such cases where upstream supplementation is possible, equity issues must be addressed. This process is similar to that used in the previous section for multiple ramp meters on a single sub-segment. First, the target ramp inflow rate for the next time interval must be calculated as:

$$\sum_{n=1}^N q_n(t-1) + q_{ramp_j}(t-1) - [\beta_i(t-1) - X_i] = F_{Total}(t) \quad (31)$$

where

n = number of metered on-ramps in the target sub-segment i

$q_n(t-1)$ = flow rate on ramp n , in the target sub-segment in the previous time interval

$q_{ramp_j}(t-1)$ = flow rate on the upstream on ramp, in the previous time interval

$\beta_i(t-1)$ = Cumulative inflow-outflow

X_i = Threshold inflow-outflow

$F_{Total}(t)$ = Target ramp inflow for the upcoming time interval

Again the ramp metering rate for each meter is based on the recent demand observation.

This consideration is similar to equation 8, except that the upstream on-ramp is included:

$$\frac{d_k(t-1)}{\sum_{n=1}^N d_n(t-1) + d_{ramp\ j}(t-1)} F_{Total}(t) = RMR_k(t) \quad (32)$$

where

k = total number of metered ramps (sum of sub-segment ramps and upstream ramp)

$d_k(t-1)$ = demand on ramp k in the previous time interval

RMR_k = demand weighted ramp metering rate for on-ramp k

It is worth noting that it is possible that a given ramp can be called for inflow control on the sub-segment for which it belongs and for supplemental inflow control for the immediate downstream sub-segment. In this case, the lower (more restrictive) ramp metering rate will be selected. Specifically, the ramp metering rate of the upstream ramp can be determined by:

$$RMR_{i+1}^{Final}(t) = \min[RMR_{i+1}(t), RMR_{i+1}^*(t)] \quad (33)$$

where

RMR_{i+1}^{Final} = selected ramp metering rate for the upstream meter

RMR_{i+1} = calculated ramp metering rate for the congested upstream sub-segment

RMR_{i+1}^* = calculated supplemental ramp metering for sub-segment i

Realizing that upstream supplementation is the limit for controlling inflow into the target sub-segment, the restrictions on metering rates below half of the maximum are lifted. However, real-time, demand-based equity considerations are still used. In the instance where the required ramp metering is below the minimum ramp metering rate, the minimum ramp metering will be selected.

As congested conditions dissipate, the cumulative inflow-outflow observation will begin to fall, as will the need to control inflow. Thus, the required ramp metering rates will gradually grow until metering is no longer needed. The sections above describe how ramp meters are activated and how the ramp metering rates are calculated and updated. The discussion now moves to the control logic for turning off ramp metering.

3.2.8. Ramp Metering De-Activation

When multiple ramps are activated to control the ramp flows into a congested sub-segment (whether it be from a sub-segment with multiple on-ramps or a supplemental upstream on-ramp), the ramps are turned off in a sequential order. Eventually, the required metering rate will be above half the maximum rate for the downstream meters. If this condition is observed for five consecutive intervals, then the farthest upstream ramp will be turned off. Each of the remaining ramps will be turned off in a similar fashion until only the most downstream on-ramp on the sub-segment remains activated.

The final ramp meter will be deactivated if the observed inflow-outflow remains below the threshold for five consecutive intervals. Recall that when the inflow-outflow drops below the threshold value, the maximum ramp metering rate is used. Thus, if the maximum ramp metering rate can consistently keep the inflow-outflow below the critical value, the system assumes that the congested period is terminating and ramp metering control is no longer needed.

3.3. Statistical Models for VSL and VSL with Ramp Metering

Benefits

3.3.1. Measures of Effectiveness for VSL Control

Before designing the experiment and gathering the data required for the development of the VSL planning tool, evaluation criteria were defined. To evaluate the impact of VSL and VSL paired with ramp metering at a given site, three MOEs were chosen to represent measures of safety, mobility, and environmental impact, respectively. As evident in the literature, observations of crashes are rare events. Furthermore, crashes cannot be represented in traffic simulation software. Thus, several surrogate measures of safety have been developed and calibrated with field observations. Among the surrogate measures of safety, speed variance has been cited as perhaps the strongest surrogate in describing increased crash risk (Garber and Gadiraju 1990, Golob et al. 2004, and Abdel-Aty et al. 2008). Thus, speed variance was selected to measure safety performance. Next, mobility was evaluated via total time spent in the network during the analysis period. This is a common mobility MOE in the literature, as it includes the impact of VSL or ramp metering on the mainline as well as the associated on-ramps.

Speed variance was calculated using 20-second volume weighted speed data from all the detectors on the study segment. Thus, the speed variance (SV) was calculated as:

$$SV = \frac{1}{IJ} \sum_{j=1}^T (v_{ij} - \bar{v})^2 \quad (34)$$

where

$$\bar{v} = \frac{1}{IJ} \sum_{i=1}^I \sum_j^J v_{ij} \quad (35)$$

I = total number of detectors

J = total number of 20-second intervals in analysis period

i = detector (1, 2, ..., I)

j = 20 second time interval (1, 2, ..., J)

Next, mobility was evaluated using total time spent by all vehicles in the network during the analysis period. The total time spent (TTS) was computed as:

$$TTS = \sum_{j=1}^J \sum_{k=1}^K \sum_{l=1}^L TT_{jkl} \quad (36)$$

where

J = Total number of 20-second intervals in analysis period

K = Total number of lanes at upstream of bottleneck

L = Total number of vehicles passing the bottleneck in lane k in time interval j

j = 20-second time interval (1, 2, ..., J)

k = lane number (1, 2, ..., K)

l = vehicle in lane k during time interval j

TT = travel time of vehicle k traveling in lane l in time period j

Having defined the specific MOEs for safety, mobility, and environmental impacts, the final step was to calculate the changes in each respective MOE under VSL or VSL paired with ramp metering control. To do so, relative changes in a given MOE were computed using the following equation:

$$\% \Delta X_i = \frac{X_{i, NoVSL} - X_{i, VSL}}{X_{i, NoVSL}} \quad (37)$$

where X_i = a given MOE ($i=1, 2, 3$)

Using normalized percent changes relative to the No VSL case offers an important advantage over the raw change in respective MOE. This advantage can be best realized using an illustrative example. Consider two candidate sites, the first with moderate speed variance before VSL control while the second has a large speed variance before VSL control. Upon evaluating VSL control at both sites, the raw changes in speed variance for both sites were found to be equal. Thus, one would conclude that in terms of speed variance, VSL control had an equal impact at both sites. However, in comparing the normalized percent change in speed variance, the moderately congested case would show a greater relative improvement to speed variance.

It is worth noting that for all three MOEs used in this study, the condition $X_{i, VSL} < X_{i, NoVSL}$ indicates that VSL control provided a benefit. Specifically, under this condition, speed variance was reduced, total time spent was reduced, or emissions were reduced. Thus, a positive $\% \Delta X_i$ value indicates that VSL control improved that respective measure.

3.3.2. Simulation Calibration

To construct the VSL planning model, a large and robust dataset was needed. However, field data for highways under VSL control are very limited. Thus, this study used VISSIM (PTV Group, 2013) traffic simulation software to develop an abundant and diverse sample of traffic environments. To estimate the impacts of VSL on the aforementioned MOEs, several scenarios were simulated with and without VSL control. As described in the following sections, the relative changes in MOEs at each scenario were used as the basis of the planning model.

The first step in developing the sample was to ensure that the simulated traffic environments reflect field observations. To do so, a field-calibrated traffic environment was used as the base scenario from which all other simulated environments were created. The site used for this calibration was the westbound direction of MD100, a four-lane, median-divided, limited access urban freeway near the Baltimore-Washington Airport with a speed limit of 55 mph (Figure 3-8). At this site, the PM peak period bottleneck occurs near the Coca-Cola Drive on-ramp (indicated by the red ring in Figure 3.1) from approximately 4:30 p.m. until 6 p.m. each weekday. This site was selected as the base site because it was used in the field-deployed VSL control study conducted by Chang et al. (2011). Thus, detailed measurements of vehicle composition, speeds, and empirical travel times were available for calibration of the base simulation environment.

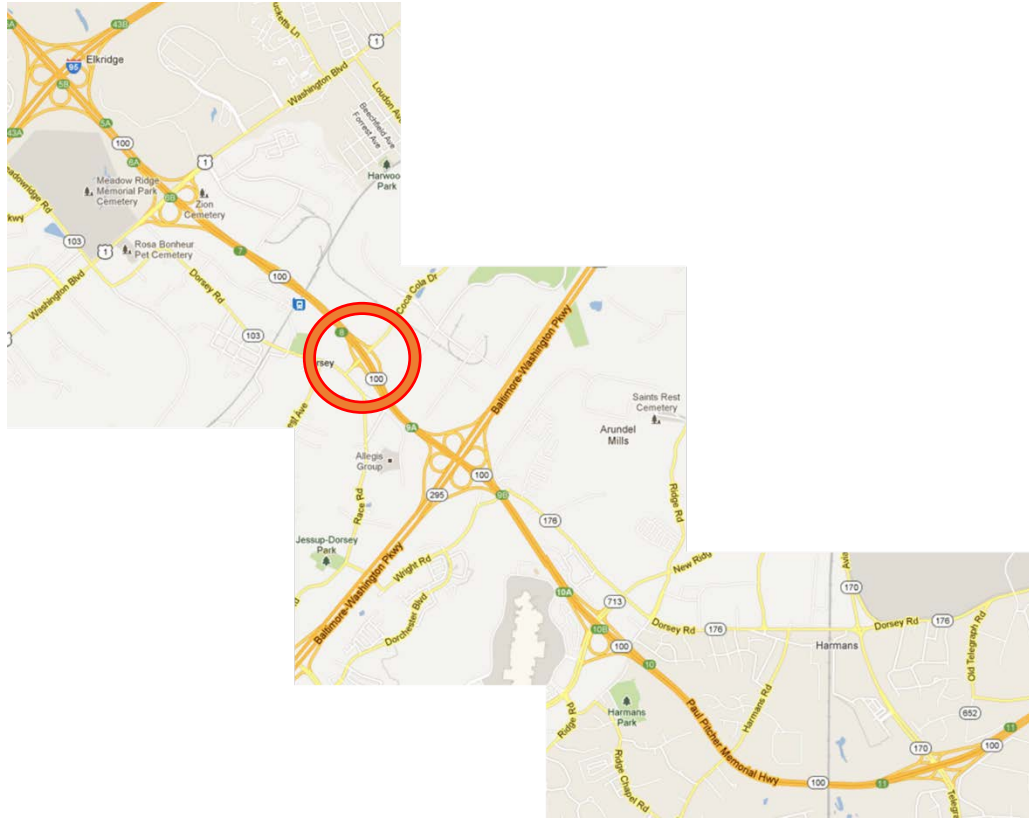


Figure 3-8: Map of Base Scenario, MD100 (Google Maps, 2013)

To ensure that the results obtained from the simulated environments reasonably reflect field conditions, data from the 2009-2010 field deployment of VSL control conducted by Chang et al. (2011) were used. The study site was located on MD100, near Baltimore, MD (Figure 5.1). MD100 is a four-lane, median-divided freeway with a posted speed limit of 55 mph. The westbound direction of this site was selected due to a recurrent afternoon peak period congestion pattern stemming from a bottleneck formed near the Coca-Cola Drive on-ramp (circled in Figure 3-8).

3.3.3. Data Set Development

In order to create a comprehensive planning tool for VSL and VSL paired with ramp metering control, a robust dataset of candidate sites must be developed. Recognizing that

datasets available for field implementation of VSL and VSL paired with ramp metering in recurrent congestion are sparse, this study turned to VISSIM (PTV Group, 2013) traffic simulation software to generate the dataset.

The first step in generating the dataset of candidate sites was to identify critical variables that may influence the impact of VSL and VSL paired with ramp metering control. The initial list of critical variables contained 11 variables, each with several possible levels. Recognizing that simulating all potential variable levels was not possible, several experimental simulation runs were conducted to identify the variables that were significant in estimating the effect of VSL and VSL paired with ramp metering in terms of total time spent and speed variance. This effort reduced the initial list of 11 variables down to 5 variables. These variables and their respective levels are presented in Table 3.1.

Table 3-1: Final List of Control Variables for Model Development

Control Variable	Variable Levels			
Distance to Upstream On-ramp (miles)	0.5	1	1.5	2
% Trucks	2.5	5	10	15
V/C at Bottleneck	0.85	0.9	0.95	1
% V/C from Bottleneck Ramp	10	15	20	25
Driver Compliance (%)	25	50	75	100

Upon identifying the factors that may affect the results of VSL and VSL paired with ramp metering control, an exhaustive list of all possible variable combinations was created in the simulation environment, resulting in 1,024 combinations. For each traffic scenario, the

simulation was run under three conditions: no control, VSL control, and VSL paired with ramp metering control. The simulated VSL and VSL paired with ramp metering control scenarios implement the algorithms proposed in chapters three and four. To reflect the natural variation in driver behavior at given sites, each simulation was run under three random seeds. Thus, a total of 9,216 total simulations were performed. The final output parameters for each simulation environment were calculated by averaging the results of each of the three random seeds. The results of these simulations were used to create the expected benefits models in terms of change in total time spent and speed variance under VSL control or VSL paired with ramp metering control relative to the no-control case. While simulation offers the advantage of creating multiple traffic scenarios, care must be taken to ensure that the results accurately estimate field conditions. To do so, this study used field observations from a VSL control pilot study. The simulation calibration effort is explained in the following section.

3.3.4. Simulation Calibration

The parameters that need to be calibrated include: transition flow weight factor α_i , congestion wave speed γ , jam traffic density d_J , critical traffic density d_C , free flow speed u_f , and traffic model parameters ν , τ , κ , a . To minimize the difference between detector measurement and model prediction results, the calibration objective is set to minimize the performance index defined below:

$$Min PI = \sum_i \sum_k \left[\left| \frac{q_i^{measured}(k) - q_i^{predicted}(k)}{q_i^{measured}(k) + q_i^{predicted}(k)} \right| + \left| \frac{u_i^{measured}(k) - u_i^{predicted}(k)}{u_i^{measured}(k) + u_i^{predicted}(k)} \right| \right] \quad (38)$$

One can then apply a Genetic Algorithm to search the optimal values of those parameters. The calibration results are listed as follows:

Table 3-2. The Calibration Results of Parameters

Parameters	Calibrated Values
α_i	0.95
γ (km/hour)	25
d_J (veh/lane/km)	120
d_C (veh/lane/km)	30
u_f (km/hour)	100
v (km ² /hour)	55
τ (seconds)	36
κ (veh/km)	40
a	2.0

For performance evaluation, the micro-simulation software VISSIM, was used as an unbiased platform to test the proposed models. Similarly, the key parameters in VISSIM were calibrated with the field data. For the car-following parameters, the maximum look ahead distance was calibrated to be 1,000 ft and the CC1 (headway time) was set as 0.80 second. Lane-changing parameters were also calibrated, where the maximum deceleration was -20.11 ft/s² for own and -19.85 ft/s² for trailing vehicle; the accepted deceleration was -8.27 ft/s² and -6.63 ft/s² for own and trailing vehicle respectively; and the waiting time before diffusion was 90 seconds.

3.3.5. VSL Benefits Models

In order to find the models that produced the most accurate prediction, several model types of varying levels of sophistication were evaluated. The first step in the planning structure is to construct a decision model. Clearly, the accuracy of the decision model affects the results in the later branches of the structure. Therefore, the accuracy of each of the following proposed decision models was compared before rules were developed for deciding if VSL improved speed variance. The next step was to develop and evaluate predictive models for VSL and VSL paired with ramp metering to estimate expected benefits from either ATMS strategy.

First, in considering the potential application of the planning tool, a hierarchical structure was created. Here, the decision maker may not need to know the exact change in safety resulting from VSL or VSL paired with ramp metering. Rather, the decision maker may only need to know if VSL control has reasonable probability of improving safety. Thus, the speed variance was discretized into three levels, No Safety Improvement, Mild Safety Improvement, and Considerable Safety Improvement. The decision to implement VSL was based on an ordered probit model for changes in safety. If safety is predicted to be improved, the model then estimates the changes in total time spent. This modeling method is presented in Figure 3-9.

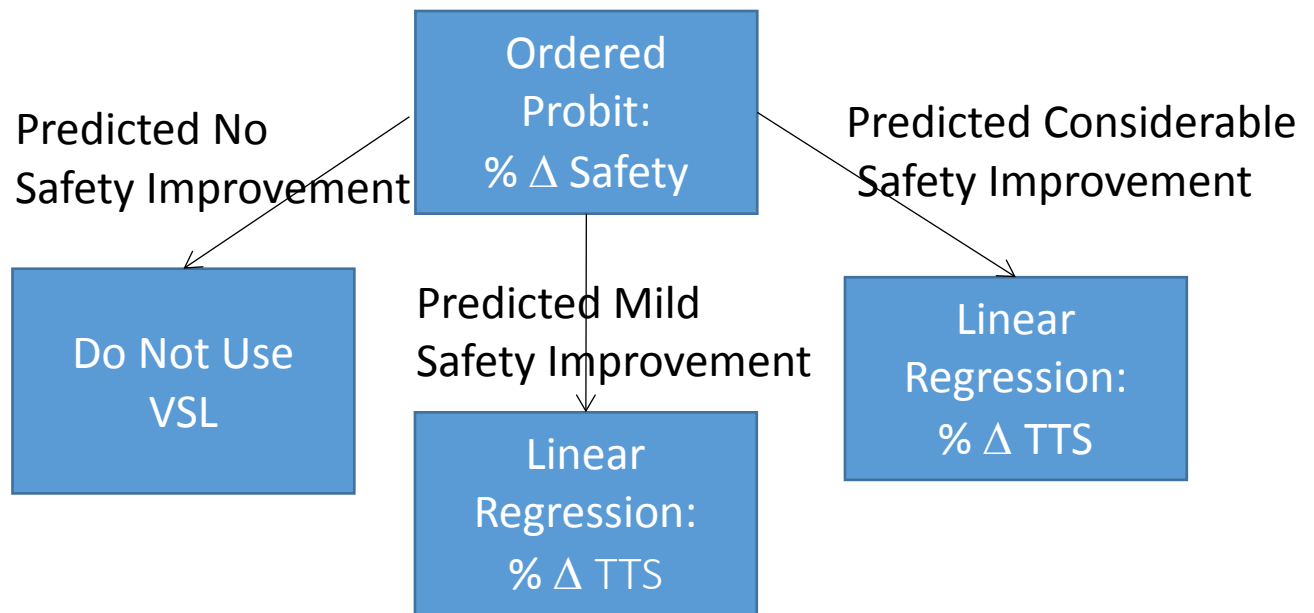


Figure 3-9: Hierarchical Structure of Planning Model

Next, a discrete continuous (DC) model was considered. Specifically, the DC model applied in this study consisted of an ordered probit discrete model for changes in speed variance and a linear regression model to predict changes in total time spent. The proposed model is a spinoff of the work by Cirillo et al. (2013). This model is supplemented by an independent linear regression model for changes in vehicle emissions from either VSL or VSL paired with ramp metering. The primary advantage of using a discrete continuous model is that both discrete and continuous models are estimated simultaneously. In doing so, errors in one model can be considered in the other model. In this particular application, errors made in the decision model can be reflected in the predictions of the effects models. The relationships between these error terms are computed by the correlation between the error terms in each model.

The first step in building the DC model was to discretize the change in speed variance, which is inherently continuous. The following discretization rules were based on the distribution of the $\% \Delta SV$ variable:

$$\text{if } \% \Delta SV \leq 0, \text{ then Bin} = 0 \quad (39)$$

$$\text{if } 0 < \% \Delta SV \leq 25, \text{ then Bin} = 1 \quad (40)$$

$$\text{if } \% \Delta SV > 25, \text{ then Bin} = 2 \quad (41)$$

where

Bin 0 = no safety improvement

Bin 1 = mild safety improvement

Bin 2 = considerable safety improvement

Next, to predict the ordered change in speed variance we define a variable (Z) that is also discretized to determine the speed variance bin. Z is defined by:

$$Z = X_{SV}^T \beta_{SV} + \varepsilon_{SV} \quad (42)$$

which was discretized by:

$$\text{If } Z < \gamma_0 \text{ then Bin} = 0 \quad (43)$$

$$\text{If } \gamma_0 < Z < \gamma_1 \text{ then Bin} = 1 \quad (44)$$

$$\text{If } Z > \gamma_1 \text{ then Bin} = 2 \quad (45)$$

From these relationships, we assume that the error term follows the standard normal distribution, $\varepsilon \sim N(0,1)$. It follows that Z follows a normal distribution, $Z \sim N(X^T \beta, 1)$. To predict the change in total time spent, linear regression was applied as:

$$Y = X_{TTS}^T \beta_{TTS} + \varepsilon_{TTS} \quad (46)$$

where

$$Y \sim N(X^T \beta, \sigma^2) \quad (47)$$

With both components of the DC model described, the joint model was developed by assuming the error terms in both components follow a multivariate normal distribution with correlation ρ . Thus, the likelihood of a given observation is:

$$p(Z, Y) = f(Y)p(Z|Y) \quad (48)$$

where

$$f(Y) = \phi(Y | X^T \beta, \sigma^2) \quad (49)$$

Given Y, the conditional probability for the error term of the ordered probit model is:

$$\varepsilon_{SV} | Y \sim N\left(\frac{p(Y - X_{TTS}^T \beta_{TTS})}{\sigma}, (1 - \rho^2)\right) \quad (50)$$

Thus:

$$p(Z|Y) = p(\gamma_i < N\left(X_{SV}^T \beta_{SV} + \frac{p(Y - X_{TTS}^T \beta_{TTS})}{\sigma}, (1 - \rho^2)\right) < \gamma_{i+1}) \quad (51)$$

The report now turns to presenting the results of the above-described methodologies.

4. Findings

4.1. Optimal VSL Control Results

As a major MOE to evaluate traffic efficiency, the time-dependent travel time can clearly reflect the effectiveness of each control strategy. Figure 4-1(A) presents the resulting travel time from these two models with the objective of minimizing travel time and the No-VSL

scenario. Notably, the travel time starts to increase when the freeway is becoming congested (after 7 a.m.). Compared with the no-control scenario, the average travel time is reduced under the KF-TTT model, demonstrating the benefits under the VSL control. However, the benefit of VSL with BASIC-TTT is not significant. The reason is that without the Kalman Filter correction, the macroscopic traffic flow model cannot fully capture the occurrence of congestion caused by traffic weaving effect at the downstream bottleneck. From Figure 4-1(B), it is clear that both speed-variance minimization models can reduce the travel time during the congested period (7 a.m.-8 a.m.). Also, the KF-SV model clearly outperforms the BASIC-SV model.

A further comparison between two KF models is shown in Figure 4-1(C). Note that during the period from 6:45-7:15 a.m., the KF-TTT model produces a lower travel time than the KF-SV model. However, as the congestion increases from 7:15 a.m., the KF-SV model begins to show better performance. To understand this interesting finding, we further analyzed the simulation process and found that the KF-SV model is more sensitive to the change in traffic conditions and it can immediately adjust the speed limit in advance even during the moderate congested period. The capability to adjust speed in time can reduce the flow rate to the downstream segments, and consequently mitigate the potential shockwave impact.

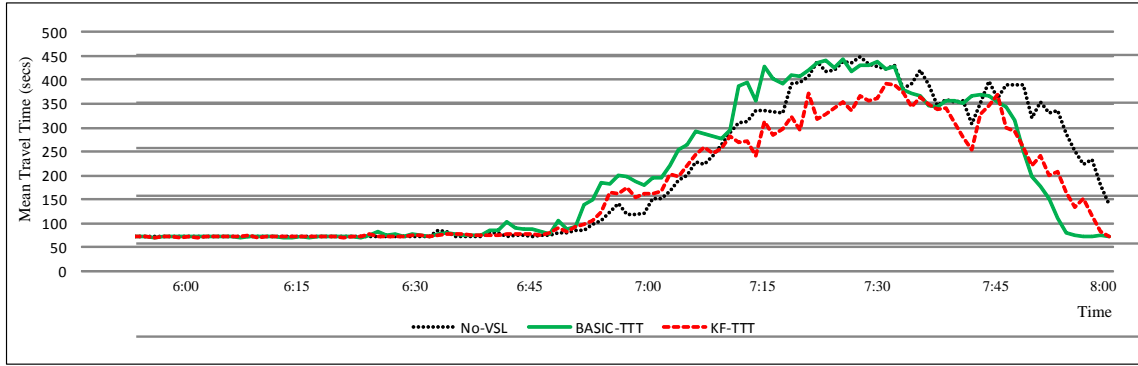


Figure 4-1(A). Time-dependent Travel Time: BASIC-TTT, KF-TTT vs. No-VSL Scenario

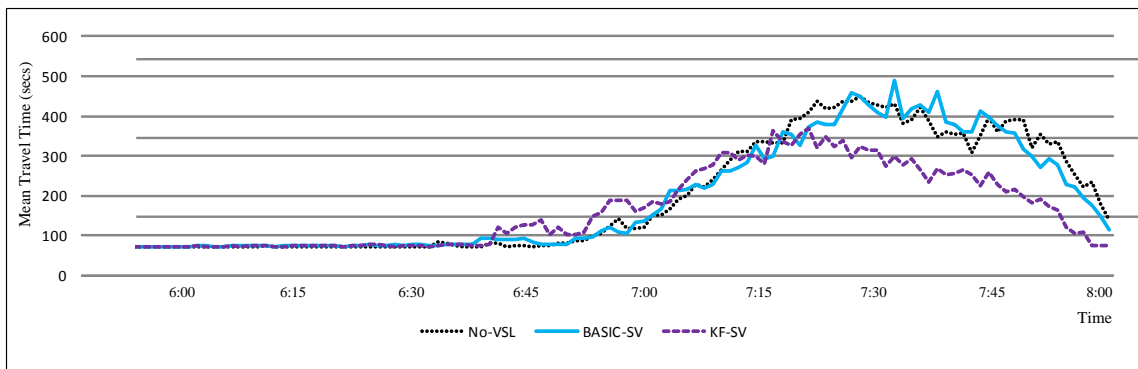


Figure 4-1(B). Time-dependent Travel Time: BASIC-SV, KF-SV vs. No-VSL Scenario

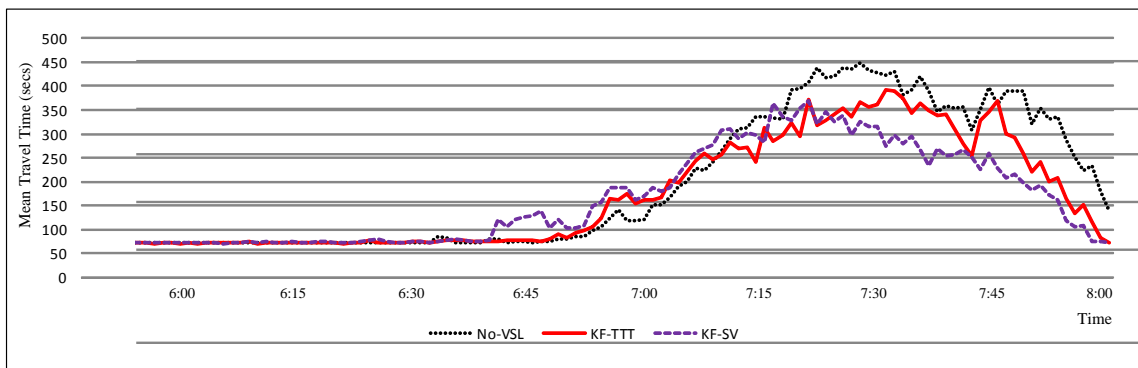


Figure 4-1(C). Time-dependent Travel Time: KF-TTT, KF-SV vs. No-VSL Scenario

As reported in the literature, an effective VSL system can reduce a driver’s “stop-and-go” frequency. Therefore, the number of vehicle stops can also be viewed as an effective MOE for evaluating the efficiency of each proposed VSL system. Figures 4-2(A) through 4-2(C)

also compare the time-dependent number of vehicle stops among different scenarios, and the results also indicate the promising property of the KF models, especially the one with the objective of minimizing speed variance (KF-SV).

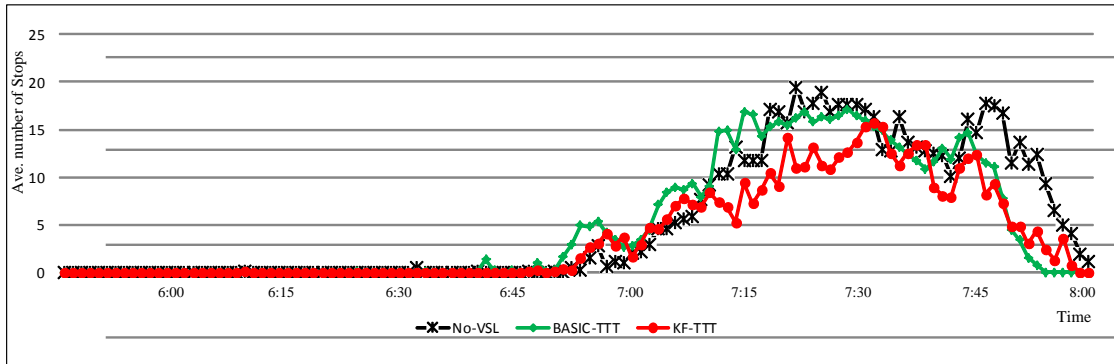


Figure 4-2(A). Time-dependent Number of Stops: BASIC-TTT, KF-TTT vs. No-VSL Scenario

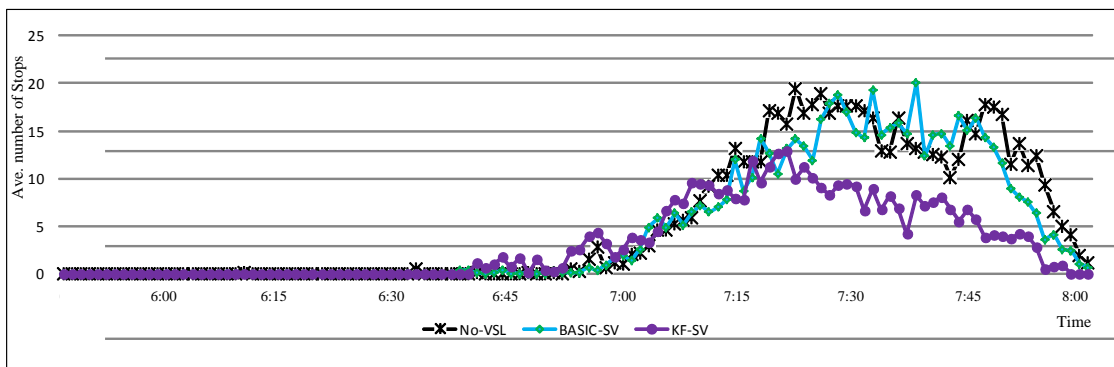


Figure 4-2(B). Time-dependent Number of Stops: BASIC-SV, KF-SV vs. No-VSL Scenario

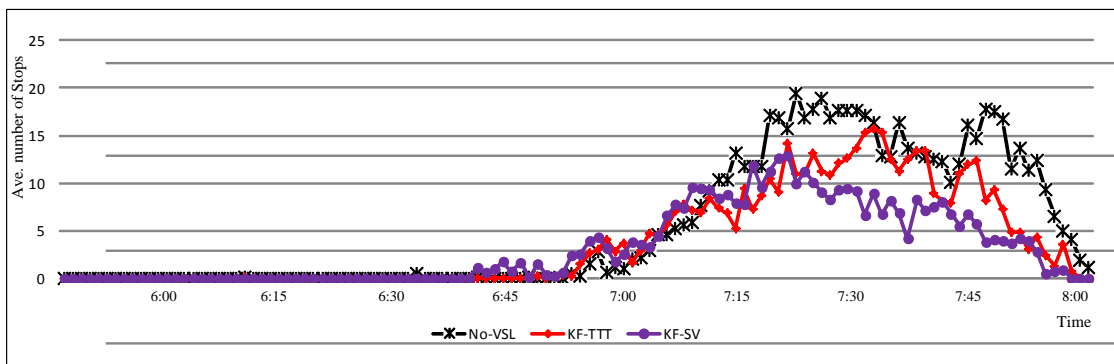


Figure 4-2(C). Time-dependent Number of Stops: KF-TTT, KF-SV vs. No-VSL Scenario

Table 4-1 summarizes the MOEs for all scenarios. To prevent the randomness of results, the data have been averaged over 10 simulation replications. Moreover, to distinguish the performance between the congested (7 a.m.-8 a.m.) and uncongested periods (6 a.m.-7 a.m.), Table 4-1 shows the overall results over the entire period and over the congested period. Notably, all proposed models can yield significant reduction in both total travel time and vehicle stops. Among those four, KF-SV model is the best, yielding a reduction of 36.6 percent on the vehicle stops and 14.7 percent on the average travel time during the 2-hour period. The KF-TTT model, with its dynamic update function, outperformed BASIC-SV and achieved a reduction in vehicle stops and travel time, respectively, by 26.9 percent and 12.6 percent.

4.2. VSL and VSL with Ramp Metering Benefits Models Results

4.2.1. Hierarchical Model Results and Analysis

The entire hierarchical model was built using SPSS (IBM, 2013) software. The first step in constructing the hierarchical model was to estimate the parameters for the ordered probit VSL control decision model using the model building subset. Using the adjusted VC ratio, speed variance under no ATMS control, and driver compliance as predictor variables, the probit equation was estimated. Table 4-2 summarizes the results of the ordered probit model. Note that Bin 0 (No Safety Improvement) was used as the reference bin.

Table 4-1. Performance Comparison between Different Scenarios

Scenario	6:00-8:00 Ave. # of		7:00-8:00 Ave. # of		6:00-8:00 Ave. Travel		7:00-8:00 Ave. Travel		Speed	
	Stops		Stops		Time (s)		Time (s)		Variance	
										(mile/hr)
No-VSL	6.34	/	10.49	/	214.6	/	302.9	/	41.3	/
BASIC-TTT	6.10	-3.79%	9.70	-7.53%	211.0	-1.68%	294.0	-2.94%	38.4	-7.0%
KF-TTT	4.63	-26.97%	7.61	-27.45%	188.5	-12.16%	257.3	-15.05%	34.1	-17.4%
BASIC-SV	5.64	-11.04%	9.30	-11.34%	209.7	-2.28%	290.3	-4.16%	37.5	-9.2%
KF-SV	4.02	-36.59%	6.33	-39.66%	183.0	-14.73%	241.9	-20.14%	31.4	-23.9%

Table 4-2: Change in Speed Variance Modeling Results in the Hierarchical Structure

	Parameter	Estimate	St. Error	Wald	Sig.
Thresholds	Bin 1 (Mild Safety Improvement)	1.164	0.425	7.50	0.006
	Bin 2 (Considerable Safety Improvement)	2.521	0.428	34.733	0.000
Predictor Variables	No Control SV	0.008	0.000	574.645	0.000
	Adj VC	0.089	0.435	0.042	0.837
	Driver Compliance	0.006	0.001	39.899	0.000

The results from Table 4-2 suggest that the changes in speed variance bins were indeed statistically significant from each other. Next, consider the sign of each variable coefficient and their respective significance. The estimate for the no ATMS control speed variance was positive and statistically significant. This finding makes sense, as one would expect that a

scenario with high-speed variance would likely have speed variance decreased under VSL control. Moving on to the adjusted VC ratio variable, the estimate was found to also be positive. However, the adjusted VC ratio proved to be insignificant in predicting change in speed variance. Though this result was not expected, further investigation revealed that the cause was related to variable selection. Specifically, the adjusted VC ratio did not significantly contribute to explaining the variance model beyond what the other predictor variables could explain. Finally, the estimate of the coefficient for driver compliance was positive and statistically significant. This finding obviously makes sense because increased driver compliance to VSL signs should improve safety benefits.

To evaluate the prediction accuracy of the model, the parameter estimates in Table 4-2 were used to compute the likelihood functions for each scenario in the validation set. To assess accuracy, it was assumed that the bin with the highest probability would be assigned as the predicted bin for each scenario. Thus, the prediction accuracy was summarized in Table 4-3.

Table 4-3: Change in Speed Variance Modeling Accuracy in the Hierarchical Structure

	SV Bin	Predicted Response % Δ SV Bin			TOTAL
		Bin 0	Bin 1	Bin 2	
Actual Response % Δ SV Bin	Bin 0 (No Safety Improvement)	16	48	7	71
	Bin 1 (Mild Safety Improvement)	15	92	28	135
	Bin 2 (Considerable Safety Improvement)	1	39	122	162
TOTAL		32	179	157	368

From Table 4-3, the overall accuracy is simply the sum of the correctly predicted scenarios over the total number of scenarios. Thus, the prediction accuracy for the change in speed variance was found to be 62.5%. However, it is worth noting that if a scenario is predicted in Bin 1 or Bin 2, it will be passed on to the VSL effects models. Under this consideration, accuracy may be alternatively defined in a pseudo-binary matter by considering the merging of Bin 1 and Bin 2 (i.e., those sites with some level of safety improvement). In doing so, the accuracy is elevated to 80.7%. Using the latter approach, 297 scenarios were passed to the VSL effects models to predict the expected changes in total time spent and emissions, independently.

Similar to the change in speed variance decision model, the VSL effects models were constructed in SPSS using an 80/20 data split for model building (238 observations) and evaluation (59 observations). Here, linear regression analysis was applied using the same three predictor variables as before: adjusted VC ratio, speed variance under no ATMS control, and driver compliance. The results of both the change in total time spent is presented in Tables 4-4.

Table 4-4: Change in Total Time Spent Modeling Results in the Hierarchical Structure

Variable	Unstandardized Coefficients		Standardized Coefficients	t	Sig.
	B	Std. Error	Beta		
No Control SV	-0.016	0.004	-0.436	-4.234	0.000
Adj VC	-.143	1.512	-0.011	-0.094	0.925
Driver Compliance	0.227	0.008	1.182	26.682	0.000

The results in Table 4-4 suggest that only two of the three predictor variables were found to be statistically significant in predicting the change in total time spent resulting from VSL

control. While the sign of the adjusted VC ratio was compatible with engineering logic, it was found to be insignificant. Similar to the decision model, the adjusted VC ratio did not contribute to explaining the variance in change in total time spent beyond what was explained by the other predictor variables. In any case, the regression coefficient for speed variance with no ATMS control was found to be negative and statistically significant. This discovery agrees with intuition, as VSL control aims to reduce speeds of vehicles upstream of the bottleneck area. Finally, the coefficient for driver compliance was positive and statistically significant. Obviously this result was expected. As more people comply to the VSL signs, the duration and severity of the bottleneck are reduced. Thus, one would expect the mobility benefits to increase with driver compliance.

The accuracy of the change in total time spent model was evaluated via the adjusted R^2 value. Here, adjusted R^2_{TTS} was found to be 0.627.

4.2.2. DC Model Results and Analysis

In this model structure, the change in emissions was estimated in an independent model. The DC model uses the methodologies of Cirillo et al. (2013) to estimate the coefficients for the order probit and continuous linear regression models along with the correlation between the error terms in both components. To carry out this analysis, a script was prepared using the R statistical package (2013). Using the same model building set as used in the hierarchical model, the DC model was constructed. The results are summarized in Table 4-5.

Table 4-5: DC Modeling Results

	Variable	β	Std. Dev.	t	Sig.
Ordered Probit Model (for % Δ SV)	Driver Compliance	0.007	0.001	7.185	0.000
	Adj VC	-.004	0.405	-0.011	0.991
	No Control SV	0.794	0.033	23.717	0.000
	α_1	1.353	0.045	30.10	0.000
Linear Regression Model (for % Δ TTS)	Driver Compliance	0.222	0.006	39.630	0.000
	Adj VC	-21.627	2.336	-9.257	0.000
	No Control SV	-0.919	0.161	-5.713	0.000
	σ^2	46.537	1.531	30.390	0.000
	ρ	0.148	0.027	5.457	0.000

Similar to the ordered probit model in the hierarchical structure, the ordered probit component of the DC model found the VC ratio to be insignificant. However, the coefficient for driver compliance was found to be both positive and significant, as expected. Next, the no-ATMS-control speed variance coefficient also followed expectations in being positive and significant.

Interestingly, in contrast to the linear regression model for total time spent in the hierarchical structure component, the analogous component of the DC models found the coefficient for the adjusted VC ratio to be statistically significant and negative in sign. Considering that this analysis only considers base VC ratios from 0.85 to 1.15, this result makes sense. As the VC ratio increases, one would expect the severity and duration of the bottleneck to increase and thus the mobility benefits under VSL control to be reduced. Next, the no-ATMS-control speed coefficient was discovered to be negative and significant in predicting the change in total time spent. As described earlier, this finding agrees with

engineering logic. Finally, as expected, the coefficient for driver compliance was positive and statistically significant.

Using the same evaluation methods used to analyze the predictive accuracy of the hierarchical model components, the accuracy of the DC model was investigated. The results of the ordered probit component of the DC model are presented in Table 4-6.

Table 4-6: DC Modeling Results

	SV Bin	Predicted Response % Δ SV Bin			TOTAL
		Bin 0	Bin 1	Bin 2	
Actual Response % Δ SV Bin	Bin 0 (No Safety Improvement)	23	28	6	57
	Bin 1 (Mild Safety Improvement)	6	107	29	142
	Bin 2 (Considerable Safety Improvement)	2	41	126	169
TOTAL		31	176	161	368

Using the results presented in Table 4.4, the overall predicted accuracy for the ordered probit model was found to be 69.6%. However, using the pseudo-binary evaluation described above, the accuracy becomes 88.6%. For the linear regression component of the DC model, an R^2 value of 0.678 was found.

5. Conclusions

5.1. Optimal VSL Control Algorithms

The basic proactive model used the embedded traffic flow relations to predict the evolution of congestion pattern and compute the optimal speed limit. To contend with the difficulty in capturing driver responses to VSL control, this study also proposed an advanced model with an embedded Kalman Filter function. Both models were investigated with different traffic conditions and control objectives. The results of extensive VISSIM simulation revealed that both proactive VSL control models can significantly reduce the travel time and the number of vehicle stops over recurrent bottleneck locations at MD 100, and the one using minimizing speed variance as its control objective clearly outperforms other models, as reflected in the performance evaluation results.

5.2. VSL Model Comparison

The results and analysis of the hierarchical and DC models for independent VSL control show that the benefits of VSL can indeed be accurately predicted. However, the ordered probit component of the DC model structure proved to produce better results in terms of overall accuracy and the pseudo-binary definition of accuracy. In fact, the ordered probit DC component outperformed its hierarchical counterpart by 7.1% in terms of overall accuracy and by 7.9% in terms of pseudo-binary accuracy. In considering the linear models for change in total time spent, the DC component showed slight improvements in the hierarchical component with an R^2 of 0.678.

The superior results produced by the DC model can be explained by the fact that the DC model simultaneously estimates the models for change in speed variance and change in total time spent resulting from VSL control. In doing so, errors made in the one model are considering in the other model. Applying the correlation between these error terms improved the predictions and model fitting in the DC model.

5. Recommendations

Despite the promising performance of our proposed models at this exploratory stage, the authors fully recognize that much remains to be done on this subject. One of our ongoing tasks is to calibrate driver response parameters based on more field data. Also, the sensitivity of model performance to the traffic measurement errors was not answered in this study. Other ongoing research tasks associated with VSL implementation include: exploring the potential of using multiple control objectives, identification of optimal detector locations for updating traffic conditions, and optimization of the number of VMS speed displays for smoothing speed transition between the free-flow and the bottleneck traffic conditions.

Next, though the VSL and VSL paired with ramp metering benefits models show promise, each needs to be validated and calibrated with field data. As many agencies are investing in ATMS strategies to mitigate congestion, more data can be collected on how VSL and ramp metering affect the safety and mobility of road users in recurrent congestion.

REFERENCES

1. Abdel-Aty, M., Pande A., and Hsia L. (2010). The Concept of Proactive Traffic Management for Enhancing Freeway Safety and Operation, *ITE Journal*, Vol. 80, Issue 4, pp. 34-41.
2. Abdel-Aty, M., Cunningham, R., Gayah, V., and Hsia, L., 2008. Dynamic Variable Speed Limit Strategies for Real-time Crash Risk Reduction on Freeways, *Journal of the Transportation Research Board*, No. 2078, pp. 108-116.
3. Abdel-Aty, M., Dilmore, J., and Hsia, L. (2006). Applying Variable Speed Limits and the Potential for Crash Migration, *Journal of the Transportation Research Record*, Vol. 1953, pp. 21-30.
4. Abdel-Aty, M., Dilmore, J., and Dhindsa, A. (2005A). Evaluation of Variable Speed Limits for Real-Time Freeway Safety Improvement. *Accident Analysis and Prevention*, Vol. 28, pp. 335-345.
5. Abdel-Aty, M., Pande, A., Lee, C., Gayah, V., and Dos Santos, C. (2007). Crash Risk Assessment using Intelligent Transportation Systems Data and Real-time Intervention Strategies to Improve Safety on Freeways, *ITS Journal*, Vol. 11, Issue 3, pp. 107-120.
6. Abdel-Aty, M., Uddin, N., Pande, A. (2005B). Split Models for Predicting Multi-vehicle Crashes during High-speed and Low-speed Operating Conditions on Freeways. *Compendium of papers CDROM, Transportation Research Board 2005 Annual Meeting*, Washington, D.C.
7. Allaby, P., Hellinga, B., and Bullock, M. (2007). Variable Speed Limits: Safety and Operational Impacts of a Candidate Control Strategy for an Urban Freeway, *IEEE Transactions on Intelligent Transportation Systems*, Vol. 8, No. 4, pp. 671-680.

8. Anund, A., and Ahlström, C. (2009). *Evaluation of Local ITS Solutions in Urban Areas*. Swedish National Road and Transport Research Institute, No. 646.
9. Barlovic, R., Santen, L., Schadschneider, A., and Schreckenberg, M. (1998). Metastable States in Cellular Automata for Traffic Flow, *The European Physical Journal B*, Vol. 5, No. 3, pp. 793-800.
10. Bellemans, T., De Schutter, B., and De Moor, B. (2003). Anticipative model predictive control for ramp metering in freeway networks. In *American Control Conference*, pp. 4077–4082, Denver, Colorado, June 2003.
11. Bertini, R., Bogenberger, K., and Boyce, S. (2005). Impact of Driver Information System on Traffic Dynamics on a German Autobahn: Lessons for U.S. Applications, 12th World Congress on Intelligent Transport Systems. 2005.
12. Bertini, R., Boice, S., and Bogenberger, K. (2006). Dynamics of Variable Speed Limit System Surrounding Bottleneck on German Autobahn. *Transportation Research Record*, No. 1978, pp. 149–159, Transportation Research Board of the National Academies, Washington, D.C.
13. Bertini, R., Hansen, S., and Bogenberger, K. (2004). Empirical Analysis of Traffic Sensor Data Surrounding a Bottleneck on a German Autobahn. Transportation Research Board 84th Annual Conference, Washington, D.C.
14. Bham, G., Long, S., Baik, H., Ryan, T., Gentry, L., Lall, K., Arezoumandi, M., Liu, D., Li, T., and Schaeffer, B. (2010). *Evaluation of Variable Speed Limits on I-270/I-255 in St. Louis*, Missouri DOT, Report No. OR 11-014.

15. Carlson, R., Papamichail, I., and Papageorgiou, M. (2011). Local Feedback-Based Mainstream Traffic Flow Control on Motorways Using Variable Speed Limits. *IEEE Transactions on Intelligent Transportation Systems*, Vol. 12, No. 4, pp. 1261-1276.
16. Chang, G. L., Park, S. Y., and Paracha, J. (2011). ITS Field Demonstration: Integration of Variable Speed Limit Control and Travel Time Estimation for a Recurrently Congested Highway. Transportation Research Board 90th Annual Conference, Washington, D.C.
17. Cirillo, C., Liu, Y., and Tremblay, J. M. (2013). Ordered and Unordered Discrete-Continuous Models: A Comparative Analysis for Household Vehicle Holding and Mileage Traveled Decisions. Transportation Research Board 92nd Annual Conference, Washington, D.C.
18. Duret, A., Ahn, S., and Buisson, C. (2012). Lane flow distribution on a three-lane freeway: General features and the effects of traffic controls. *Transportation Research Part C*, Vol. 24, pp. 157-167.
19. Fuhs, C. (2010). *Synthesis of Active Traffic Management Experiences in Europe and the United States*. Federal Highway Administration Report FHWA-HOP-10-031.
20. Garber, N. J., and Gadiraju, R. (1990). Factors influencing speed variance and its influence on accidents. *Transportation Research Record*, Vol. 1213, pp. 64-71.
21. Geistefeldt, J. (2011). Capacity effects of variable speed limits on German freeways. *Procedia Social and Behavioral Sciences*, Vol.16, pp. 48-56.
22. Ghods, H., Fu, L., and Kian, A. R. (2010). An Efficient Optimization Approach to Real-Time Coordinated and Integrated Freeway Traffic Control, *IEEE Transactions on Intelligent Transportation Systems*, Vol. 11, No. 4, pp. 873-884.

23. Grumert, E., Ma, X. and Tapani, A. (2013). Effects of a Cooperative Variable Speed Limit System on Traffic Performance and Exhaust Emissions. Transportation Research Board 92nd Annual Conference, Washington, D.C.
24. Hegyi, A. (2004). Model Predictive Control for Integrating Traffic Control Measures. Doctoral Dissertation. Delft University of Technology, Netherlands. 2004.
25. Hegyi, A., De Schutter, B., and Hellendoorn, J. (2005A). Optimal Coordination of Variable Speed Limits to Suppress Shock Waves, *IEEE Transactions on Intelligent Transportation Systems*, Vol. 6, No. 1, pp. 102-112.
26. Hegyi, A., De Schutter, B., and Hellendoorn, H. (2005B). Model Predictive Control for Optimal Coordination of Ramp Metering and Variable Speed Limits. *Transportation Research Part B*, Vol. 13C, No. 3, pp. 185-209.
27. Hegyi, A., Hoogendoorn, S. (2010). Dynamic speed limit control to resolve shock waves on freeways – Field test results of the SPECIALIST algorithm. Annual Conference on Intelligent Transportation Systems, Madeira Island, Portugal.
28. Heydecker, B. G., and Addison, J. D. (2011). Analysis and modeling of traffic flow under variable speed limits. *Transportation Research Part C*, Vol. 19, pp. 206–217.
29. Highway Agency Publications Group (2007). *Summary Report: M25 Controlled Motorways*. Bristol, UK.
30. Hoogerndoom, S. P., Daamen, W., Hoogendoorn, R. G., and Goemans, J. W. (2013). Assessment of Dynamic Speed Limits on Freeway A20 near Rotterdam, the Netherlands. Transportation Research Board 92nd Annual Conference, Washington, D.C.
31. Jiang, R., Chang, E., and Lee, J. (2011). Variable Speed Limits: Conceptual Design for Queensland Practice. Australian Transport Research Forum, Adelaide, Australia.

32. Kerner, B. and Klenov, S. (2002). A Microscopic Model for Phase Transitions in Traffic Flow. *Journal of Physics A: Mathematical and General*, Vol. 35, No 3, pp. L31-L43.
33. Kerner, B. and Rehborn, H. (1997). Experimental properties of phase transitions in traffic flow, *Physical Review Letters*, Vol. 79, No. 20, pp. 4030-4033.
34. Kianfar, H., Edara, P., and Sun, C. (2013). Operational Analysis of a Freeway Variable Speed Limit System- Case Study of Deployment in Missouri. Transportation Research Board 92nd Annual Conference, Washington, D.C.
35. Krajzewicz, D. (2010). Traffic Simulation with SUMO - Simulation of Urban Mobility. In J. Barceló (Ed.), *Fundamentals of Traffic Simulation* (Vol. 145, pp. 269-293), New York Dordrecht Heidelberg London: Springer.
36. Kwon, E., Park, C., Lau, D. and Kary, B. (2011A). Minnesota Variable Speed Limit System: Adaptive Mitigation of Shock Waves for Safety and Efficiency of Traffic Flows. Transportation Research Board 90th Annual Conference, Washington, D.C.
37. Kwon, E., Park, C., Lau, D., Kary, B. (2011B). Development and field assessment of variable advisory speed limit system. In: Proceedings of the 18th ITS World Congress, Orlando, Florida.
38. Lee, C., Saccomanno, F., and Hellinga, B. (2002). Analysis of Crash Precursors on Instrumented Freeways. In *Transportation Research Record*, Vol. 1784, pp. 1-8.
39. Lee, C., Hellinga, B., and Saccomanno, F. (2003). Real-time crash prediction model for application to crash prevention in freeway traffic. *Transportation Research Record*, Vol. 1840, pp. 67-77.
40. Lee, C., Hellinga, B., and Saccomanno, F. (2004). Assessing Safety Benefits of Variable Speed Limits. *Transportation Research Record*, Vol. 1897, pp. 183-190.

41. Lee, C., Hellinga, B., Saccomanno, F. (2006). Evaluation of variable speed limits to improve traffic safety. *Transportation Research Part C*, Vol.14, pp. 213-228.
42. Hasan, M. (1999). Evaluation of Ramp Control Algorithms Using Microscopic Traffic Simulation, Master of Science Thesis, MIT.
43. Messner, A., and Papageorgiou, M. (1990). METANET: A macroscopic simulation program for motorway networks. *Traffic Engineering & Control*, Vol. 31, No.1, pp. 466-470.
44. Mirshahi, M., Obenberger, J., Fuhs, C., Howard, C., Krammes, R., Kuhn, B., Mayhew, R., Moore, M., Sahebjam, K., Stone, C., and Yung, J. (2007). *Active Traffic Management: The Next Step in Congestion Management*. Federal Highway Administration Report No. FHWA-PL-07-012, Washington, D.C.
45. Nes, N., Brandenburg, S., and Twisk, D. (2010). Improving homogeneity by dynamic speed limit systems. *Accident Analysis and Prevention*, Vol. 42, pp. 944-952.
46. Nissan, A., and Koutsopoulos, H. (2011). Evaluation of the impact of advisory variable speed limits on motorway capacity and level of service. *6th International Symposium on Highway Capacity and Quality of Service Procedia Social and Behavioral Sciences*, Stockholm, Sweden, pp. 100-109.
47. Papageorgiou, M., Kosmatopoulos, E., and Papamichail, L. (2008). Effects of Variable Speed Limits on Motorway Traffic Flow. *Transportation Research Record*, Vol. 2047, pp. 37-48.
48. Popv, A., Hegyi, A., Babuska, R., and Werner, H. (2008). Distributed Controller Design Approach to Dynamic Speed Limit Control Against Shockwaves on Freeways. *Transportation Research Record*, Vol. 2086, pp. 93-99.
49. PTV Group (2013). VISSIM Micro-Simulation Software.
50. Quadstone Limited (2002). PARAMICS Modeler. Edinburgh, UK.

51. R Development Core Team (2008). *R: A language and environment for statistical computing*. R Foundation for Statistical Computing, Vienna, Austria. ISBN 3-900051-07-0, URL <http://www.R-project.org>.
52. Robinson, M. (2000). Examples of Variable Speed Limit Applications. Prepared for the Speed Management Workshop at Transportation Research Board 79th Annual Conference, Washington, D.C.
53. Sailer, H., Schoepf, K. F., and Kühne, R. D. (1997). Speed Limit Effects on the Multilane Traffic Flow through a Bottleneck. *Proc., 8th International Federation of Automatic Control Symposium*, Chania, Greece, pp. 1289-1294.
54. Shi, H., and Ziliaskopoulos, A. (2002). Traffic Flow Control using Variable Speed Limits. *Traffic and Transportation Studies*, 2002, pp. 658-665.
55. Smulders, S. (1990). Control of Freeway Traffic Flow by Variable Speed Signs. *Transportation Research Part B*, Vol 24B, No. 2, pp. 111-132.
56. Ibid.
57. Smulders, S. (1992). Control by variable speed signs – the Dutch experiment, in *Proceedings of the Sixth International Conference on Road Traffic Monitoring and Control*, IEE Conference Publication, London, pp. 99-103.
58. Steel, P., and McGregor, R. (2005). Application of Variable Speed Limits along the Trans Canada Highway in Banff National Park. Annual Conference of the Transportation Association of Canada, September 2005, Calgary, Canada.
59. Stoelhorst, H., Schreuder, M., Polderdijk, S., Wilmink, I., Jonkers, E. (2011). Summary results of Dutch field trials with dynamic speed limits (dynamax). In: *Proceedings of the 18th ITS World Conference*, Orlando, Florida.

60. Transport Simulation Systems (2013). Aimsun. Barcelona, Spain.
61. Ulfarsson, G., Shankar, V., Vu, P., Mannering, F., Boyle, L. and Morse, M. (2001). *In-Vehicle Signing and Variable Speed Limit Evaluation*. Washington State Transportation Center Report No. T9903. Seattle, WA.
62. Wang, Y., Ioannou, P. (2011). A New Model for Variable Speed Limits. Compendium of papers CDROM, Transportation Research Board 2011 Annual Meeting, Washington, D.C.